NOVEMBER 10 2025

Asymmetric temporal envelope encoding: Lateralization with varying envelope shape and spectral mismatch

Sean R. Anderson ; Alan Kan ; Matthew J. Goupell ; Ruth Y. Litovsky

J. Acoust. Soc. Am. 158, 3724–3743 (2025)
https://doi.org/10.1121/10.0039519

JASA ARTICLE

Asymmetric temporal envelope encoding: Lateralization with varying envelope shape and spectral mismatch

Sean R. Anderson,[1,a)] Alan Kan,[2] Matthew J. Goupell,[3] and Ruth Y. Litovsky[1]
[1]Waisman Center, University of Wisconsin-Madison, Madison, Wisconsin 53705, USA
[2]School of Engineering, Macquarie University, New South Wales, Australia
[3]Department of Hearing and Speech Sciences, University of Maryland, College Park, Maryland 20742, USA

ABSTRACT:
Bilateral cochlear implants (BiCIs) improve spatial-hearing outcomes relative to a single cochlear implant (CI), but the extent varies across patients. One limiting factor may be interaurally asymmetric spectro-temporal representations of sounds. The present study simulated interaural spectro-temporal asymmetries to explore how they affect binaural processing in listeners with normal hearing. We simulated CI stimulation using high-rate (500 pps) band limited acoustic pulse trains with a 3 mm bandwidth and 4 or 6.5 kHz center frequency. Second-order amplitude modulation (AM) was applied at a 100 Hz modulation rate, 20% or 50% modulation depth, and sinusoidal or sawtooth shape. Intracranial lateralization was used to assess utility of whole-waveform interaural time differences (ITDs). Results demonstrated that lateralization of envelope ITDs was limited by the ear with smaller AM depth. This effect depended upon the sharpness of temporal onsets and the extent to which frequencies overlapped in each ear. These results suggest that interaural asymmetry in spectro-temporal representations may limit binaural outcomes of patients with BiCIs. Two well-established models of binaural processing that assume interaural symmetry and rely on coincidence-detection were used to predict performance. Models were mostly predictive of performance, but made consistent errors, suggesting that models of BiCI stimulation using coincidence-detection should be improved to account for asymmetries. https://doi.org/10.1121/10.0039519

(Received 20 December 2024; revised 14 July 2025; accepted 4 September 2025; published online 10 November 2025)

[Editor: Christopher A. Brown] Pages: 3724–3743

NOMENCLATURE

AM	Amplitude modulation
BiCI	Bilateral cochlear implant
CI	Cochlear implant
EE	Excitatory-excitatory
EI	Excitatory-inhibitory
ENI	Electrode-neuron interface
ILD	Interaural level difference
ITD	Interaural time difference
LSO	Lateral superior olive
MSO	Medial superior olive
NH	Normal hearing
pps	Pulses per second
SAM	Sinusoidally amplitude modulated

I. INTRODUCTION

Binaural cues provide essential information for listeners to determine the location of a sound source in the horizontal plane and distinguish target speech from background noise (Litovsky *et al.*, 2021). These cues consist of interaural time differences (ITDs) and interaural level differences (ILDs). Listeners with normal hearing (NH) rely more heavily upon ITDs at low frequencies to localize broadband sound sources (Macpherson and Middlebrooks, 2002). Further, listeners derive greater advantage when target and masking sounds are spatially separated if ITDs are provided compared to ILDs (Bronkhorst and Plomp, 1988; Ihlefeld and Litovsky, 2012; Swaminathan *et al.*, 2016). The benefits of ITDs to listeners with NH have motivated researchers over the years to attempt to provide ITDs via cochlear-implant (CI) processors and improve ITD sensitivity, but listeners with bilateral cochlear implants (BiCIs) demonstrate extraordinary variability with respect to their sensitivity to ITDs. This occurs even under ideal stimulus conditions when the timing of pulses to electrodes in the two ears is carefully controlled, and loudness balanced stimuli are used (e.g., Cleary *et al.*, 2022; Thakkar *et al.*, 2020). Many factors are thought to limit access to ITDs conveyed via bilateral CIs (BiCIs), and thus, sensitivity to ITDs in BiCI users; these include hardware and software limitations, as well as patient histories.

One factor that may limit performance with BiCIs is the presence of interaurally asymmetric encoding of temporal information (Anderson *et al.*, 2022; Ihlefeld *et al.*, 2015), which has rarely been studied or modeled in listeners with NH (Anderson *et al.*, 2019b; Anderson *et al.*, 2023). Models of BiCIs have been used to make predictions about factors that limit outcomes with BiCIs or improvements that can be made to technology (Dietz, 2016), suggesting that accounting for these asymmetries could lead to better binaural hearing for listeners with BiCIs. The present studies investigated

[a)]Email: sean.hearing@gmail.com

whether simulated interaural temporal asymmetries lead to reduced ITD lateralization range. The experiments in the present paper used 500 pps acoustic pulse trains that simulate pulsatile stimulation with a CI. In experiment 1 (Sec. II), the proof of concept was tested using sinusoidally amplitude-modulated (SAM) pulse trains with symmetric or asymmetric amplitude modulation (AM) depth. In experiment 2 (Sec. III), the interaction of interaural temporal asymmetries and attack time of the temporal envelope was investigated using sawtooth modulators. In experiment 3 (Sec. IV), the interaction of interaural temporal asymmetries and interaural place-of-stimulation mismatch was investigated. Data were compared against predictions from existing models of binaural processing that have demonstrated high predictive accuracy in listeners with NH presented with interaurally symmetric stimuli.

A. Binaural processing in NH

1. Basics and limitations

Sensitivity to ITDs depends upon the parameters of the stimulus. One example is sensitivity to ITDs in the temporal fine structure, which is greater for low frequencies and formed the basis of "duplex theory" of sound source localization (i.e., ITDs are only used to localize low-frequency sounds) (Lord Rayleigh, 1907). Listeners with NH only show sensitivity to fine-structure ITDs below 1500 Hz (e.g., Klug and Dietz, 2022; Zwislocki and Feldman, 1956). Envelope ITDs can be used at higher carrier frequencies above 1500 Hz (e.g., Bernstein and Trahiotis, 2002). In this case, we consider the basilar membrane as a frequency analyzer, where the "temporal fine-structure" refers to the carrier that is modulated by another signal, the "temporal envelope" (Moore, 2008).

CIs use electrical pulses delivered to specific portions of the auditory nerve. When listeners with NH or BiCIs are presented with pulsatile and spatially selective stimulation, ITD sensitivity declines above rates of 300 Hz (e.g., Anderson *et al.*, 2019a; Majdak *et al.*, 2006). ITD sensitivity is also greater for stimuli with a sharp envelope attack time in listeners with NH (e.g., Bernstein and Trahiotis, 2002; Klein-Hennig *et al.*, 2011; Laback *et al.*, 2011). Increasing bandwidth also leads to increased ITD sensitivity when stimuli have sharp temporal envelopes (Goupell *et al.*, 2013b; Mayo *et al.*, 2021). Thus, it is important to control for bandwidth when completing studies on the role of envelope sharpness.

CI processors are able to represent ITDs via amplitude-modulated pulse trains (Kan *et al.*, 2018), suggesting that they can be useful under ideal circumstances. All experiments in the present study used amplitude-modulated trains of band limited acoustic pulses in an effort to simulate CI stimulation. (See the supplementary material for example waveforms of stimuli used in each experiment) Two temporal features were manipulated. In all experiments, the AM depth was presented at 20% or 50%, representing poor (20%) or good (50%) temporal fidelity. In experiments 1 and 3, sinusoidal modulators were used. In experiment 2 (Sec. III), sawtooth ("ramped") or reversed sawtooth ("damped") modulators were used. Because the modulator was simply reversed, the magnitude spectrum and therefore bandwidth remains the same, allowing experiment 2 to remove confounds of bandwidth and focus on modulator sharpness. In experiment 3, spectral features were manipulated. The center frequency was varied independently in each ear to simulate interaural place-of-stimulation mismatch and control for effects of center frequency.

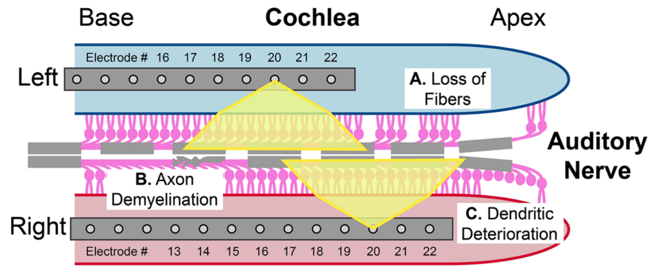

FIG. 1. Illustration of the electrode-neuron interface (ENI). This illustration shows examples of factors that can affect the spectro-temporal representations of sounds in each ear for listeners with BiCIs.

2. Lateral superior olive (LSO) and medial superior olive (MSO)

Briefly, the firing rate of cells in the MSO varies with fine-structure ITDs (Yin and Chan, 1990) and MSO cells are mostly tuned to lower frequencies (Guinan *et al.*, 1972). Further, MSO cells have a "best delay" to which they are most responsive, which is thought to correspond to a characteristic delay in the arrival of inputs from the ipsilateral and contralateral ear to the action potential initiation site (for review, see Joris and van der Heijden, 2019). Cells in the MSO act as coincidence detectors (Golding and Oertel, 2012), responding when excitatory input from the ipsilateral and contralateral ear arrive within a given time window. They are accordingly referred to as excitatory-excitatory (EE) cells. This is an oversimplification as it is well known that inhibition plays a key role in the MSO (Brand *et al.*, 2002). When decoding the relationship between neural responses and spatial cues, there is evidence to suggest that the difference in rate between the two hemispheres may play a key role in mammals (McAlpine and Grothe, 2003), sometimes referred to as the rate difference model.

The firing rate of the LSO varies with envelope ITDs (e.g., Joris and Yin, 1995) and LSO cells are mostly tuned to higher frequencies (Guinan *et al.*, 1972). Arrays of many CIs tend to be shallowly inserted into the cochlea, stimulating the cells in the high-frequency region. Cells in the LSO receive excitatory input from the ipsilateral ear and inhibitory input from the contralateral ear (Boudreau and Tsuchitani, 1968; Franken *et al.*, 2018; Tollin and Yin, 2002) and are therefore referred to as excitatory-inhibitory (EI) cells. This means that LSO cells modify their output depending upon the amount of coincidence and are least responsive when sounds arrive with a contralaterally leading

250 μs ITD. LSO responses increase on average as the ITD increases or decreases from 250 μs. Thus, poorer envelope encoding in either ear has been associated with decreased ITD sensitivity in NH (Anderson *et al.*, 2019b; Bernstein and Trahiotis, 2011) and BiCIs (Anderson *et al.*, 2022; Ihlefeld *et al.*, 2014).

Critically, both MSO and LSO cells have extremely short (sub-millisecond) time constants, meaning that their spike rate is only modulated when the timing of inputs is highly coordinated (Brown and Tollin, 2016; Franken *et al.*, 2018; Golding and Oertel, 2012). This sensitivity is accomplished by precise encoding of temporal information prior to binaural computations, which occurs for the fine structure and temporal envelope. A detailed review of binaural circuits is provided by Yin *et al.* (2019).

B. Binaural processing in BiCIs

1. Limitations (processors, rate limitations, interaural place mismatch, electrode-to-neural interface)

Most modern sound processing algorithms in CIs disregard the temporal fine structure of a sound (Loizou, 2006). The low-passed temporal envelope is conveyed, meaning that only ITDs in the slower fluctuations of amplitude over time are conveyed (Gray *et al.*, 2021). In addition, these listeners do not rely on ITDs for sound source localization (Aronoff *et al.*, 2010; Fischer *et al.*, 2021; Grantham *et al.*, 2008). Because BiCIs are not interaurally coordinated in commercially available sound processors, binaural cues are poorly represented or distorted. For example, automatic gain control and uncoordinated CI clocks may lead to the introduction of ITDs that do not correspond to the stimulus being presented (Dennison *et al.*, 2022; Gray *et al.*, 2021). Even when CI coding strategies do provide temporal fine structure information, their utility may be limited to narrowband low-frequency signals (e.g., Fischer *et al.*, 2021; Zirn *et al.*, 2016). Envelopes are represented by a series of electrical pulses whose amplitudes correspond to the dynamic range (i.e., softest and loudest sounds a listener with BiCIs can tolerate) and can thus differ between the ears. A smaller dynamic range limits sensitivity to spatial cues (Ihlefeld *et al.*, 2014; Todd *et al.*, 2017), which we simulate in the present study by reducing the depth of AM.

Listeners with BiCIs are further limited by temporal aspects of CI stimulation. Most of the research concerning ITD sensitivity has used low-rate ($\sim$100 pps) pulsatile stimulation, which tends to yield optimal sensitivity to ITDs in listeners with NH (Anderson *et al.*, 2019a; Bernstein and Trahiotis, 2002, 2009) and BiCIs (Anderson *et al.*, 2019a; Kan and Litovsky, 2015; Laback *et al.*, 2015). When using controlled and bilaterally synchronized direct stimulation and low rates ($<$300 Hz) in the temporal envelope, listeners with BiCIs demonstrate sensitivity to static (e.g., Anderson *et al.*, 2019a; Noel and Eddington, 2013; van Hoesel *et al.*, 2009) and dynamic envelope ITDs (better performers only) (Anderson *et al.*, 2022). Listeners with NH and BiCIs also show reduced sensitivity for rates below 100 Hz when stimuli are amplitude modulated (Anderson *et al.*, 2019a; Noel and Eddington, 2013). In listeners with NH, this decrease in sensitivity has been related to the sharpness of onset of the envelope (e.g., Klein-Hennig *et al.*, 2011). However, the only study to date that controlled for off-time and sharpness of the envelope in listeners with BiCIs did not show improved sensitivity to sharp envelopes. That study also showed improved sensitivity with increasing off-time (Laback *et al.*, 2011). This final point is particularly important for understanding the stimuli to which a listener may retain ITD sensitivity and how CI processing strategies may be able to most effectively convey ITDs.

Temporal and spectral factors may interact. Many CIs stimulate with electrical pulses corresponding to different frequencies than those stimulated with NH. Further, interaural place-of-stimulation mismatch occurs when electrodes corresponding to the same frequency information (i.e., frequency allocation table or bandpass cut-off frequencies) stimulate different regions of the cochlea in each ear. Interaural place-of-stimulation mismatch leads to impacts on ITD discrimination and lateralization. Lateralization represents the extent to which listeners perceived a sound at particular locations to the left and right inside of their head when binaural cues, in this case ITDs, are varied. Presentations of stimuli in these types of experiments tend not to be externalized (i.e., are perceived inside of the head) presumably because of the lack of spectral cues that listeners typically use (Best *et al.*, 2020). A greater range of lateralization responses implies that spatial cues are more useful to perceiving locations. In contrast, a smaller lateralization range implies ITDs are not very useful or influential on perception. Large interaural place-of-stimulation mismatch can occur. for instance, if CI surgery in the two ears does not ensure the same insertion depth of the two electrodes (Cleary *et al.*, 2022). Studies that deliberately manipulate interaural mismatch found poorer sensitivity to ITDs (Cleary *et al.*, 2022; Kan *et al.*, 2015; Poon *et al.*, 2009) and smaller lateralization range (Kan *et al.*, 2013; Kan *et al.*, 2019) with increased interaural mismatch. In listeners with NH, stimuli that produce interaural place-of-stimulation differences also lead to poorer sensitivity to ITDs conveyed in the temporal envelope (Blanks *et al.*, 2007; Blanks *et al.*, 2008; Goupell *et al.*, 2013b; Henning, 1974; Nuetzel and Hafter, 1981) and smaller lateralization ranges (Goupell *et al.*, 2013b; Kan *et al.*, 2013; Kan *et al.*, 2019). Interaural frequency mismatch also leads to a smaller component of the auditory brainstem response that reflects binaural interaction in animals (Brown *et al.*, 2019) and humans with NH (Sammeth *et al.*, 2023).

Spectral and temporal factors also affect the "fusion" of binaural percepts (for a detailed review, see Reiss and Goupell, 2024), or the tendency of listeners to perceive a single sound image for bilaterally presented stimuli. Stimuli with large frequency differences are often perceived as two distinct spatial objects for listeners with NH (e.g., Goupell *et al.*, 2013b; Kan *et al.*, 2013; Kan *et al.*, 2019). Temporal asymmetries have been explored to a lesser extent. Recent studies with BiCIs and simulations suggest that differences in temporal fidelity may affect the ability to appropriately group sounds together when they are the same or segregate them when they are different (Anderson *et al.*, 2019b; Anderson *et al.*, 2022; Anderson *et al.*, 2023), and that sensitivity to spatial cues is reduced when the ears have differing sensitivity to temporal cues [a behavioral proxy of the electrode-neuron interface (ENI)] (Ihlefeld *et al.*, 2015; Todd *et al.*, 2017). For a review on the relationship between different kinds of interaural asymmetry and fusion (see Anderson *et al.*, 2024). Fusion and sensitivity to spatial cues are thought to be related.

Temporal limitations and spectral factors can be understood under one overarching concept, the ENI, or the relationship between CI electrodes that stimulate auditory nerve fibers to convey auditory information to the brain (for review, see Bierer, 2010). While many studies investigating the role of the ENI in patient outcomes focus upon unilateral stimulation, differences between the ears likely play a role in binaural outcomes, generating different kinds of asymmetries between the ears. Sensitivity to ITDs has been shown to vary considerably across individuals, and relates to ENI, which varies from patient to patient (e.g., Anderson *et al.*, 2022; Cleary *et al.*, 2022; Ihlefeld *et al.*, 2015; Litovsky *et al.*, 2010; Thakkar *et al.*, 2020). Figure 1 shows some examples of problems with the ENI that may affect spectral and temporal representations of binaural cues (especially ITDs). These consist of factors that lead to spectral and temporal asymmetries.

2. ENI

Because listeners with BiCIs receive processed stimulation, they may not be limited by the same physiological factors as listeners with NH. For example, they show little to no consistent difference in sensitivity to ITDs depending upon the stimulating electrode region, which activates different auditory nerve fiber populations (Anderson *et al.*, 2022; Cleary *et al.*, 2022; Laback *et al.*, 2015; Thakkar *et al.*, 2020). Auditory nerve fibers are stimulated in a frequency selective manner with NH because of the frequency tuning of the basilar membrane.

For listeners with CIs, hair cells are bypassed and auditory nerve fibers instead phase lock to pulsatile electric stimulation up to around 1000 pps (Dynes and Delgutte, 1992). Each problem associated with the ENI, shown in Fig. 1, is expected to cause issues with phase locking and ITD encoding. For example, uniform (Nadol, 1997) or site-specific losses (Shannon *et al.*, 2002) of auditory nerve fibers limit the number of auditory nerve fiber inputs provided to the binaural pre-processors in the cochlear nucleus, which rely on oversampling of inputs to retain their improved phase locking before reaching binaural cells (e.g., Rothman *et al.*, 1993). Similarly, axon demyelination leads to poorer phase locking in models of auditory nerve fibers (Resnick *et al.*, 2018). Deterioration of dendrites leads to an increase in the latency of the action potential in model auditory nerve fibers (Goldwyn *et al.*, 2010), and could thus introduce stimulus-independent ITDs to neural responses. Collectively, these would result in temporal degradations in the stimulus, which may lead to interaural temporal asymmetry.

Thus, listeners with BiCIs likely experience a large amount of interaural temporal asymmetry that must be navigated by the binaural system, thereby limiting its performance and potentially increasing listening effort. For example, loss of auditory nerve fibers, axon demyelination, and dendritic deterioration have been related to the duration of deafness during studies of human temporal bones (Spoendlin and Schrott, 1989) and in animal models of hearing loss (Leake and Hradek, 1988; Zhou *et al.*, 1995a; Zhou *et al.*, 1995b). Increasing duration of deafness results in a deterioration of the auditory periphery (Shepherd and Hardie, 2001), worsening the ENI. Many listeners with BiCIs are implanted during adulthood and may receive their CIs sequentially (Holder *et al.*, 2018; Peters *et al.*, 2010), suggesting that the duration of deafness differs for each ear. Further, loudness growth depends upon the electrode being stimulated in listeners with BiCIs (Bierer and Nye, 2014; Fu, 2005; Kirby *et al.*, 2012), as does the ILD resulting in a centered sound image (Fitzgerald *et al.*, 2015; Goupell *et al.*, 2013a). Together, these studies suggest that for envelope ITDs with interaural temporal asymmetry, inputs to binaural nuclei may be interaurally decorrelated, resulting in a diffuse sound image (Whitmer *et al.*, 2014), poorer sensitivity to ITDs (Buchholz *et al.*, 2018; Saberi *et al.*, 1998), and poorer spatial unmasking of speech (Swaminathan *et al.*, 2016). Moreover, the extent of this effect depends upon the stimulus. High-rate pulse trains modulated by second-order AM with a sharp attack time are thought to initiate "looks" of the NH binaural system to ITDs in the stimulus (Hafter and Buell, 1990; Stecker, 2018). Sharp-onset envelopes also improve sensitivity to ITDs for high-frequency amplitude-modulated tone bursts (Dietz *et al.*, 2015; Klein-Hennig *et al.*, 2011). While listeners with BiCIs have not shown effects of sharp temporal onsets on ITD sensitivity for higher rates (Laback *et al.*, 2011), they do show evidence of a reliance on pulses at the onset of high-rate constant-amplitude stimuli (van Hoesel, 2008) and stronger weighting of other pulses across the stimulus at lower pulse rates (Hu *et al.*, 2017) (see discussion in Stecker *et al.*, 2021).

3. Models

The role of the MSO and LSO in encoding binaural cues for listeners with BiCIs remains contested in the literature (for review, see Dietz, 2016). Both EE and EI type models have successfully predicted binaural performance using stimuli that are relevant for listeners with CIs, such as trains of high-frequency acoustic transients (e.g., Bernstein and Trahiotis, 2011, 2014; Brown *et al.*, 2019; Klug *et al.*, 2020). Most modeling studies have used stimuli with interaural temporal symmetry. Thus, one important dimension that remains unexplored is interaural temporal asymmetry, as well as its interaction with interaural place-of-stimulation mismatch.

C. Summary and hypotheses

In summary, sensitivity to binaural cues might be limited by interaural temporal asymmetries in listeners with BiCIs (Anderson *et al.*, 2022; Ihlefeld *et al.*, 2015) and simulations in NH (Anderson *et al.*, 2019b). Interaural temporal asymmetries are presumably mediated by differences in the ENI in each ear and could be compounded by spectral asymmetries introduced by interaural place-of-stimulation mismatch (Fig. 1). Specifically, the input to the MSO and LSO is the cochlear nucleus, which may have greater temporal stochasticity in BICIs since improving temporal precision at this stage requires numerous healthy auditory nerve inputs. This will generate greater neural interaural decorrelation, which is detrimental to binaural processing (Buchholz *et al.*, 2018; Saberi *et al.*, 1998). To simulate asymmetric temporal encoding, second-order AM depth was decreased *in one ear* (Anderson *et al.*, 2019b). Reduced AM depth of acoustic stimuli leads to decreased phase locking in nerve recordings (Joris and Yin, 1992) and in models of the auditory nerve (Zilany *et al.*, 2014). Thus, it was hypothesized that if the second-order AM depth was decreased in one *or* both ears, envelope ITDs would be lateralized to a lesser extent, and that performance would be similar if one or both ears was stimulated with lower AM depth (experiment 1, Sec. II). It was also hypothesized that AM depth would have multiplicative effects with shallow envelope attack (experiment 2, Sec. III) and interaural place-of-stimulation mismatch (experiment 3, Sec. IV) because these stimulus parameters can also increase the amount of interaural decorrelation.

II. EXPERIMENT 1: SYMMETRIC VS ASYMMETRIC AM DEPTH

A. Motivation

The goal of experiment 1 was to determine whether lateralization of a sound is limited by the ear with smaller AM depth. Thus, three experimental conditions were devised: conditions with 50% AM depth in both ears (50%:50%), 20% AM depth in both ears (20%:20%), and an interaural temporal asymmetry condition with 20% AM depth in one ear and 50% AM depth in the other ear (20%:50%). The 20% and 50% AM depth were used to avoid floor or ceiling effects. These were the same AM depths tested by Anderson *et al.* (2019b) using SAM tones.

B. Methods

1. Listeners

Ten listeners with NH participated in this experiment (ages 19–29 years; mean age: 21.9 years). All listeners had hearing thresholds ≤20 dB hearing level for octave frequencies between 0.25–8 kHz, with no difference in threshold between the left and right ear greater than 10 dB at any frequency. Before participating in the experiment, all listeners provided informed consent. All procedures were approved by the Health Sciences Institutional Review Board of the University of Wisconsin–Madison.

2. Stimuli and equipment

Stimuli were Gaussian-enveloped tones with a center frequency of 4 kHz and second-order sinusoidal AM. Briefly, Gaussian-enveloped tones were generated by creating a train of Gaussian pulses and multiplying the result by a sine wave of the desired duration and center frequency. More details regarding Gaussian-enveloped tones can be found in Goupell *et al.* (2010) and Goupell *et al.* (2013b). The stimuli used in the present experiment were generated at a rate of 500 pps with a 3 mm bandwidth [i.e., –3 dB at ±1.5 mm from the area of peak stimulation along the cochlea (Greenwood, 1990)] or 1.74 kHz for a Gaussian-enveloped tone with a center frequency of 4 kHz. Stimuli had a duration of 500 ms. Then, second-order sinusoidal AM was applied by multiplying the constant-amplitude pulse train using Eq. (1):

$$y(t) = \left(1 + \frac{m}{100}\sin(2\pi f_m t)\right)x(t), \tag{1}$$

where $y(t)$ is the instantaneous amplitude of the SAM pulse train at time t, m is the modulation depth (ranging from 0% to 100%, and set either to 20% or 50%), f_m is the modulation frequency fixed at 100 Hz, and $x(t)$ is the instantaneous amplitude of the Gaussian-enveloped tone pulse train at time t. Stimuli were presented at 65 dB sound pressure level A-weighted [dB(A)]. Stimuli were gated with 10 ms cosine ramps at stimulus onset and offset. Whole-waveform ITDs of 0, ±100, ±200, ±400, or ±800 μs were then applied. Whole-waveform ITDs would preserve ITDs in the temporal fine structure. However, sensitivity to and lateralization of high-rate (∼500 pps) acoustic pulse trains is poor (Bernstein and Trahiotis, 2011, 2014; Monaghan *et al.*, 2015; see also the Appendix). The stimuli used in these experiments were meant to be more relevant for listeners who use BiCIs in the real world, whose auditory system is usually not stimulated at rates below 300 pps and only receive envelope ITDs through their clinical processors (Gray *et al.*, 2021). Finally, 61 dB(A) uncorrelated masking noise that began 100 ms prior to stimulus onset and persisted until 100 ms post stimulus offset was provided to prevent listeners from exploiting low-frequency non-linear distortions, which could be used as fine-structure ITD cues (Klein-Hennig *et al.*, 2011). The noise was low-pass filtered with two cutoff frequencies: the first at 200 Hz where the roll-off was −3 dB/octave and the second at 1000 Hz where the roll-off was −18 dB/octave. The AM depth in each ear is described as 20%:20%, 20%:50%, or 50%:50% depth, where, for convenience, the lower depth is shown on to the left of the colon. In the 20%:50% condition, the ear with smaller depth could have been in the left or right ear and was counterbalanced across listeners.

Stimuli were presented through insert earphones (ER-2, Etyomotic, Elk Grove Village, IL). They were generated in MATLAB (Mathworks, Natick, MA) and presented using a Tucker-Davis Technologies System3 (Tucker-Davis Technologies, Alachua, FL) System3 with digital processor, amplifier, and attenuator (RP2.1, HB7, and PA5 units, respectively). All testing took place in a double-walled, sound-attenuating booth (Industrial Acoustics Company, Inc., Naperville, FL).

3. Procedure

All listeners were familiarized with the lateralization task prior to beginning the experiment. Stimuli for the familiarization task had 50%:50% AM depth. First, listeners were shown an illustration of the graphical user interface (a cartoon face) used to judge the intracranial location of sounds similar to Litovsky *et al.* (2012). Second, the experimenter pressed buttons on the computer screen further to the left or right inside of the cartoon face, spanning from the left to the right ear, resulting in the presentation of sounds with a left- or right-leading ITD, respectively. Third, listeners were then allowed to present differing ITDs to themselves using the same buttons until satisfied and encouraged to compare ITDs near 0 μs (i.e., lateralized closer to the center of the head and therefore more difficult to distinguish). Fourth, listeners were then given a pre-test where the experimenter presented stimuli with left- or right-leading ITDs and asked listeners to verbally indicate the side on which the sound was perceived. The ITD was progressively reduced by the experimenter after each right answer. Finally, listeners were tested with five repetitions of 0 and $\pm 800\,\mu$s ITDs in random order. In this case, the ITDs presented were determined randomly by a computer program. Buttons on the user interface were replaced with a slider. Listeners could repeat the stimuli as many times as desired. If they used approximately half of the range of the slider, then they proceeded to the rest of the experiment. This criterion was used based on the experience of the experimenters. That is, sometimes when listeners are first tested, they tend to be conservative and report all stimuli as being in the center of the head. If they used less than half of the slider, they were tested with five repetitions of 0, ± 800, and $\pm 1600\,\mu$s ITDs, and then again with 0 and $\pm 800\,\mu$s ITDs. For all listeners when testing began, their lateralization range was at least approximately 50%. All testing was completed where ITDs were randomized and participants responded on the slider with the same cartoon face in the background.

Throughout the rest of testing, 20 repetitions per ITD were collected for 50%:50%, 20%:50%, and 20%:20% AM depth. Half of listeners were tested with 20% AM depth in the left ear for interaurally asymmetric conditions, and the other half with 20% AM depth in the right ear (both denoted 20%:50% throughout this report). The order of conditions was blocked by AM depth configuration and counterbalanced across listeners. This resulted in a total of 20 repetitions $\times$ 9 ITDs $\times$ 3 AM depth conditions $=$ 540 trials, which were completed in approximately 2 h. Listeners were allowed to repeat stimuli as many times as desired and submit final answers before beginning the next trial. Listeners were allowed to respond with multiple source locations. Only 0.5% of trials across all listeners included responses with multiple sources perceived; for those trials, only the most prominent source as indicated by the listener was considered during analysis.

When AM depth is small, auditory nerve fibers demonstrate poorer phase locking to the temporal envelope (e.g., Joris and Yin, 1992). To motivate the stimuli used in this study, Fig. 2 shows the degree of phase locking of model auditory nerve fibers from Bruce *et al.* (2018) to a 4 kHz center frequency (CF) pulse train with sinusoidal AM depth (the stimuli used in experiment 1) at several AM depths. As documented elsewhere (e.g., Klug *et al.*, 2020), model and physiological vector strength are best off-frequency, consistent with Fig. 2. This modeling suggests that phase locking to the second-order modulator (i.e., the temporal envelope of the acoustic pulse train) decreases with decreasing AM depth. That is, smaller AM depth leads to poorer encoding of the second-order modulator.

4. Analysis

Listeners' response locations for each stimulus were converted into numerical values within the linear range of ± 10 according to linear spacing on the slider, corresponding to the left (negative) and right (positive) sides, with 0 being the center.

Lateralization responses were fit using the function described in Eq. (2):

$$Lat(ITD) = A \,\mathrm{erf}\left(\frac{ITD - \mu_{ITD}}{\sqrt{2}\sigma}\right) - \mu_{Lat}, \quad (2)$$

where *Lat(ITD)* corresponds to the predicted value of lateralization at a particular ITD, *A* corresponds to maximum extent of lateralization achieved by the fit, erf corresponds to the error function, which takes as input any real number and whose output is bounded between ± 1, *ITD* corresponds to the value of the ITD in μs, μ_{ITD} corresponds to the horizontal shift (i.e., along the x or ITD axis), σ is related to the slope of the lateralization function, and μ_{Lat} corresponds to the vertical shift (i.e., along the y or lateralization axis). All curve fitting was completed using non-linear least squares via the curve fitting toolbox in MATLAB. (See the supplementary material for an example of fitted curves, figures, and additional appendixes.)

The lateralization range, or extent to which listeners perceived an intracranial sound at locations between the left and right ears, was assessed to provide a proxy of the impact of spatial cues on perception. Lateralization range was calculated as the absolute difference of the perceived left and right positions for each listener's fitted results, or output of the models discussed in Sec. II B 5, for ITD values of $\pm 800\,\mu$s. Lateralization ranges were assessed using a mixed-effects analysis of variance (ANOVA) model in version 1.1–21 of the lme4 package (Bates *et al.*, 2015) in *R* version 4.2. AM depth (20%:20%, 20%:50%, and 50%:50%), and all possible interactions were included as fixed-effects in the model. A random intercept associated with listener was also included. All *post hoc* paired comparisons were completed using *t*-tests and estimated-marginal

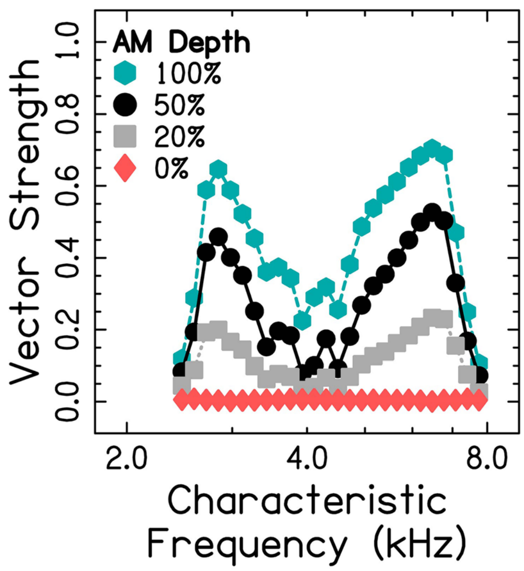

FIG. 2. Phase locking of model auditory nerve fibers. Medium spontaneous rate auditory nerve fibers (Bruce *et al.*, 2018) were used to predict changes in phase locking with varying AM depth of high-rate amplitude-modulated acoustic pulse trains based on 10 000 simulations. The *x* axis corresponds to the characteristic frequency of each fiber. The *y* axis corresponds to the vector strength (Goldberg and Brown, 1969). Different shapes correspond to the AM depth of the second-order modulator as described in the figure legend. (See also the supplementary material for further characterization of stimuli and auditory nerve model behavior.)

means with Tukey adjustments for multiple comparisons in the *emmeans* package in version 3.6.0 of *R*. Degrees of freedom were estimated with Kenward-Roger approximation (Kenward and Roger, 1997) in the *lmerTest* package of *R*.

5. Modeling

Two computational models of binaural processing were used to predict lateralization performance. They were chosen because they: (1) have been highly effective at predicting lateralization of trains of high-frequency acoustic transients, (2) represent EE- (MSO-like) and EI-type (LSO-like) binaural processing, (3) represent the two predominant decoding scheme hypotheses (place-based and rate-difference-based coding of spatial cues), (4) are available via open-source software, and (5) are computationally efficient.

The first implementation was provided by the open-source code[1] described in Akeroyd (2003). The Akeroyd implementation is a frequency- and delay-weighted version of the Jeffress model (Jeffress, 1948), where delayed copies of the signal in each ear are compared and a correlation is computed. In other words, it computes a frequency-weighted cross correlation function, and the centroid of this cross correlation is then regressed against the data observed in an experiment. The implementation used in the present study involved the cross-product rather than cross correlation (i.e., a normalized version of the cross-product). The particular parameters chosen for the Akeroyd implementation used in the present experiment were motivated by the models used in Bernstein and Trahiotis (2002, 2012). Their studies measured sensitivity to and lateralization of transient high-frequency stimuli similar to those used in the present experiment, except that our stimuli included second-order AM. The parameters are summarized in Table I. Frequency weighting functions from Stern *et al.* (1988) were used. They increase with increasing frequency until there is a peak of 600–700 Hz. Delay-weighting functions from Stern and Shear (1996) were used, which resulted in the greatest weight for ITDs near 0 μs and decreasing weights as ITDs approach larger positive or negative values. The "v = 3" transduction option was chosen to ensure that the correct frequency-weighting and delay-weighting functions could be used (Stern *et al.*, 1988 and Stern and Shear, 1996, respectively).

The second model implementation was provided in the supplementary code accompanying Klug *et al.* (2020). The Klug implementation is based upon processing in the LSO of the brainstem, where the input from the ipsilateral side is excitatory and contralateral side is inhibitory. Processing in the LSO results in sensitivity to ITDs for high-frequency stimuli (e.g., Joris and Yin, 1995), which can be modeled by counting the number of coincident spikes in a given time window (Ashida *et al.*, 2016). The parameter defaults recommended in the paper and provided in their code were used. Klug *et al.* (2020) showed a small improvement in the modeling of the data from Bernstein and Trahiotis (2012) in their original paper. Thus, both the Akeroyd and Klug implementations were ideal candidates for modeling the behavioral results in the present study; the Akeroyd implementation represents a form of EE and Klug implementation represents a physiologically based form of EI.

Model performance was assessed based on three criteria: (1) Variance explained in psychophysical data (R^2) provided a quantitative assessment, (2) the shape of the lateralization functions was qualitatively assessed, and (3) the relative change in lateralization range across stimulus parameters was also qualitatively assessed.

C. Results

1. Behavioral results

Results are shown on average and for individuals in Fig. 3(A) in percent. Lateralization responses were recorded as a score between −10 (leftmost) and +10 (rightmost). To calculate the lateralization range, the difference was taken from the curve-fitted values at +800 μs and −800 μs, then divided by 20 (the maximum). There was a significant effect of AM depth [$F(2,18) = 7.693$, $p < 0.01$]. *Post hoc* comparisons revealed that lateralization range was significantly larger for 50%:50% compared to 20%:50% [$t(18) = 2.320$, $p < 0.01$], as well as 50%:50% compared to 20%:20% AM depth [$t(18) = 3.139$, $p < 0.05$]. There was no significant difference between 20%:50% and 20%:20% AM depth [$t(18) = -0.468$, $p = 0.887$].

2. Modeling

The Akeroyd implementation predictions fit to the data had an adjusted $R^2 = 0.949$. Thus, it was highly accurate at

https://doi.org/10.1121/10.0039519

TABLE I. Akeroyd implementation parameters. These parameters are specified in the "mcorrelogram" function in MATLAB.

Parameter	Value
Lower frequency (Hz)	2000
Upper frequency (Hz)	8000
Filters per equivalent rectangular bandwidth (ERB)	1
Lower ITD (μs)	−2000
Upper ITD (μs)	2000
Transduction	"v = 3" [halfwave rectification + power-law (×^{3}) expansion of waveform]
Binaural switch	Cross product

predicting the lateralization responses averaged across listeners. The Klug implementation predictions fit to the data had an adjusted $R^2 = 0.786$. Lateralization ranges were computed in the same fashion for the model predictions as for behavioral data (see Sec. II B 4) and are shown in Fig. 3. Figure 3(C) shows exaggerated effects from the Klug compared to the Akeroyd implementation, although for both models, the direction of trends for symmetric AM depth were in line with behavioral results. Interestingly, both model implementations predicted a slightly larger lateralization range for the 20%:50% compared to the 20%:20% AM depth conditions (a normalized difference of 0.11 for Akeroyd and 0.20 for Klug), in contrast to the behavioral data.

D. Discussion

Results from experiment 1 demonstrate an important proof-of-concept for lateralization of high-rate amplitude-modulated pulse trains. That is, if *one* ear had smaller AM depth, which reduced phase locking of model auditory nerve fibers (Fig. 2), lateralization range decreased. These results, combined with those from listeners with NH (interaural envelope phase sensitivity) (Anderson *et al.*, 2019b) and BiCIs (interaural envelope phase and ITD sensitivity) (Anderson *et al.*, 2022; Ihlefeld *et al.*, 2015), provide evidence that the ear with poorer temporal representations limits binaural processing. The present study expands on the previous results by demonstrating that this limitation does not extend solely to discrimination, but to the utility of ITDs on affecting perception (i.e., lateralization). Results are consistent with previous studies using SAM stimuli showing that sensitivity to envelope ITDs or interaural envelope phase decreases as the AM depth in both ears (Bernstein and Trahiotis, 2011; Nuetzel and Hafter, 1981; Stellmack *et al.*, 2005) or one ear (Anderson *et al.*, 2019b) decreases. The present study expands these results to amplitude-modulated acoustic pulse trains.

The Akeroyd implementation was accurate at predicting mean performance of the lateralization function across listeners. The Klug implementation over-estimated lateralization of the largest ITDs, exaggerating effects of AM depth. Both model implementations predicted smaller lateralization ranges associated with reduced AM depth in one or both ears. Interestingly, both models predicted a slightly larger lateralization range for 20%:50% compared to 20%:20% AM depth. This suggests that both models were able to account for some of the decrease in lateralization range due to asymmetric AM depth, but lateralization range is overestimated relative to symmetric conditions. This finding is explored in more detail in Sec. V C.

III. EXPERIMENT 2: INTERACTIONS WITH ENVELOPE SHAPE

A. Motivation

In everyday listening, the waveforms of the sounds that we localize vary in their shape. That is, some sounds with characteristic envelope shapes may be easier to lateralize than others. Examples include transients and sounds with sharp attack times (Bernstein and Trahiotis, 2011; Dietz *et al.*, 2015), like the beat of a reverberant drum compared to a bowed violin string.

In the literature so far, there has been a divergence in the results of listeners with NH and BiCIs with respect to envelope shape. For listeners with NH, the sharper the envelope onset, the more sensitive they tend to be to binaural cues

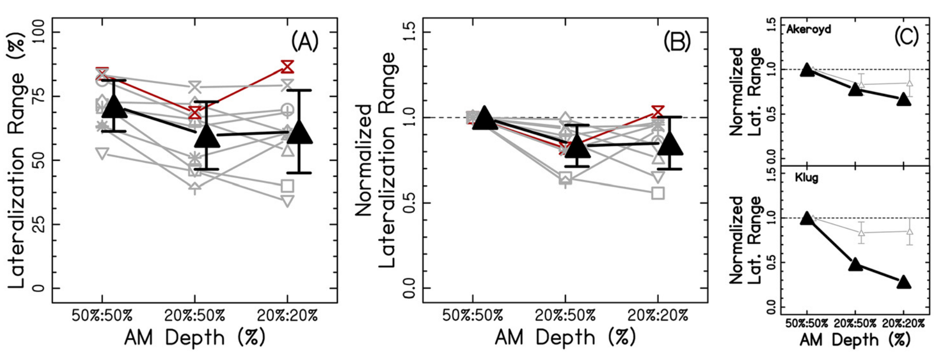

FIG. 3. Lateralization range by AM depth. The *x* axis corresponds to the AM depth, and the *y* axis corresponds to the lateralization range. (A) Raw and (B) normalized mean data ± 1 standard deviation are shown in black. Individual performance is shown offset in gray or red. Listeners (shown in red) had a lateralization range that was greater than that observed with 50%:50% for 20%:50% or 20%:20% AM depth (contrary to hypotheses). Lateralization ranges were normalized to 50%:50% AM depth. (C) Predictions from models of binaural processing. Lateralization ranges were normalized to 50%:50% AM depth. The means from (B) are shown in gray within (C) for comparison to model outputs.

(e.g., Bernstein and Trahiotis, 2002; Laback *et al.*, 2011). Listeners with BiCIs were not affected by the sharpness of the envelope (Laback *et al.*, 2011), although there are not many published studies on this topic. The shift toward listening to the peak of amplitude-modulated stimuli in listeners with BiCIs and listeners with NH at high rates (Hu *et al.*, 2017) raises the question of whether lateralization of amplitude-modulated acoustic pulse trains is affected by envelope shape for listeners with NH. It is possible that this divergence in performance is due to the use of high-rate pulsatile stimulation for BiCI and not NH, differences in AM depth, or both.

In experiment 2, we explored the relationship between different envelope shapes and interaurally asymmetric AM depth. Manipulating AM depth has the added benefit of simulating a mismatch in dynamic range between the two ears, which has been shown to have an impact on sensitivity to binaural cues (Todd *et al.*, 2017). Thus, to gain insight into how the use of onset and offset cues might be affected by differences in dynamic range between ears, and to gain a clearer understanding of the impact of interaurally asymmetric temporal fidelity on a wider set of listeners' experiences, experiment 2 evaluated two different envelope shapes with sharp or shallow attack times and identical magnitude spectra.

B. Methods

The same ten listeners who participated in experiment 1 participated in experiment 2, using the same equipment and procedures. The only exception was that sawtooth waves were used as second-order modulators instead of sine waves (for illustration of these shapes, see Fig. 4 and the supplementary material).

Two envelope shapes were tested. The first used a normal sawtooth wave with an onset linearly increasing in amplitude until a sharp offset, referred to throughout the rest of the present manuscript as a ramped envelope. The second condition was a time-reversed version of the first, such that the onset of each cycle had a sharp attack with a sloping offset and was referred to as damped. These naming conventions were adopted from Dietz *et al.* (2015). Time-reversal of one signal ensured that the amplitude spectra of both stimuli would be identical and that only the phase spectra would differ, ruling out the potential for spectral cues (e.g., bandwidth) to explain the difference between envelope conditions. Testing consisted of 20 repetitions × 9 ITDs × 3 AM depths × 2 envelope shapes = 1080 trials and took place over approximately 4 h.

C. Results

1. Behavioral results

Lateralization range is shown in Fig. 4. Average results are shown in Fig. 4(A), and individuals are shown in Fig. 4(B). It was hypothesized that lower AM depth in at least one ear and ramped compared to damped envelopes would result in reduced lateralization range. Model predictions are shown in Fig. 4(C). There was a significant effect of AM depth [$F(2,45) = 8.161$, $p < 0.001$], but not envelope type [$F(1,45) = 3.139$, $p = 0.083$]. There was a significant AM depth × envelope shape interaction [$F(2,45) = 5.262$, $p < 0.01$]. *Post hoc* comparisons revealed that, for ramped stimuli, there were no significant differences between AM depth conditions. For damped stimuli, lateralization range was greater for 50%:50% compared to 20%:50% [$t(45) = 5.051$, $p < 0.0001$], but not 50%:50% compared to 20%:20% AM depth [$t(45) = 2.269$, $p = 0.228$] or 20%:50% compared to 20%:20% AM depth [$t(45) = 2.870$, $p = 0.065$]. Additionally, the lateralization range was significantly larger for 50%:50% in the damped vs ramped conditions [$t(45) = 3.324$, $p < 0.05$].

2. Modeling

The Akeroyd implementation predictions fit to the data had an adjusted R^2 of 0.885. The Klug implementation fit to

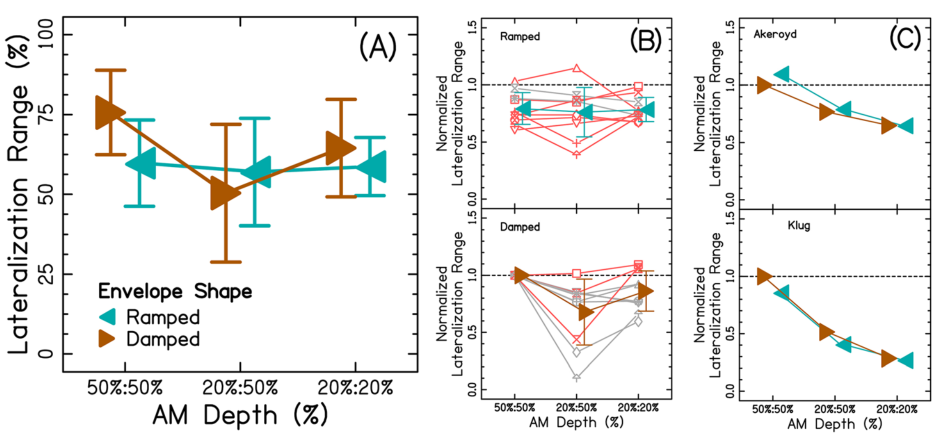

FIG. 4. Lateralization range by envelope shape and AM depth. The *x* axis corresponds to the AM depth, and the *y* axis corresponds to the lateralization range. (A) Average data ± 1 standard deviation. (B) Individual performance is shown offset in gray or red. Listeners (shown in red) had a lateralization range that was greater than that observed with 50%:50% for 20%:50% or 20%:20% AM depth (contrary to hypotheses). The top and bottom row show "ramped" and "damped" stimuli, respectively. Lateralization ranges were normalized to the damped envelope at 50%:50% AM depth. (C) The top and bottom row show model predictions for the Akeroyd and Klug implementations, respectively. Lateralization ranges were normalized to the damped envelope at 50%:50% AM depth.

the data had an adjusted R^2 of 0.743. Figure 4(C) shows that both model implementations correctly predicted that lateralization range was larger for damped compared to ramped envelopes. However, both implementations predicted effects of AM depth on lateralization range for the ramped stimuli, which is inconsistent with behavioral performance. Model predictions of lateralization range for symmetric AM depth with damped stimuli from both model implementations are consistent with behavioral performance, but consistent with experiment 1, both model implementations predicted slightly larger lateralization ranges with 20%:50% compared to 20%:20% AM depth.

D. Discussion

Experiment 2 investigated the interactions between interaurally symmetric or asymmetric temporal fidelity (i.e., AM depth) and sharp (damped) vs shallow (ramped) attack times in stimulus envelopes for high-rate amplitude-modulated band limited acoustic pulse trains. We hypothesized that ramped stimuli would show greater reductions in lateralization range for the 50%:50% AM depth conditions relative to other AM depths. Ramped stimuli tended to show the smallest lateralization ranges, but larger lateralization range for damped compared to ramped stimuli were only present at the largest AM depth. The results demonstrated an interaction between envelope shape and AM depth in the opposite direction to that hypothesized, where only stimuli with a sharp attack time (damped) demonstrated reduced lateralization range with decreasing AM depth in one ear. Interestingly, an effect of AM depth with damped stimuli was only observed between 50%:50% and 20%:50% AM depth.

Two studies investigated ITDs conveyed in amplitude-modulated high-rate pulse trains for listeners with NH (Hu *et al.*, 2017; Stecker, 2018). Stecker (2018) used SAM wideband clicks at a rate of 500 pps, varied the ITD for each click in the stimulus, and asked listeners to report the perceived position of sounds. Then, a temporal weighting function (i.e., regressed the perceived location against the ITD for each click in the stimulus) was calculated to determine which clicks in the stimuli influenced the listeners' perceived location. Results showed that clicks at the onset were most highly weighted, regardless of the rate of sinusoidal AM (31.25, 62.5, and 125 Hz or constant amplitude). Hu and colleagues measured ITD discrimination for 200 or 600 pps, band limited acoustic pulses with a center frequency of 0.2, 0.6, or 4 kHz and sinusoidal AM (Hu *et al.*, 2017). The AM rates used in their experiment were 2 or 8 Hz. Their results demonstrated similar discrimination accuracy for onset and peak of the stimulus for the 200 pps pulse train, whether ITDs were presented via fine-structure or envelope. For the 600 pps pulse train, discrimination performance was more accurate for ITDs in the onset of the sound. Broadly speaking, both studies are in agreement with the psychophysical literature demonstrating that high-rate (∼500 pps) constant-amplitude band limited acoustic pulse trains result in a weighting of the onset of a sound (e.g., Hafter and Dye, 1983). The results from Stecker (2018) suggest that the slope of the onset of a click train should not affect onset weighting, and the results of Hu *et al.* (2017) suggest that onset-weighting probably depends upon the pulse rate of the amplitude-modulated pulse train.

The present study is consistent with the notion that ITDs are sampled during transient increases in the temporal envelope for high-rate stimulation, when "enveloped-triggered looks" to ITDs are initiated ("restart" hypothesis) (Hafter and Buell, 1990; Stecker, 2018). The lateralization range of 500 pps constant-amplitude pulse train is similar to that of the multiple shallow "onsets" (ramped) stimulus at all AM depths tested and the multiple sharp onsets (damped) stimulus with smaller AM depth in one ear (see the Appendix). Thus, the present study shows that lateralization of envelope ITDs using high-rate amplitude-modulated pulse trains depends upon AM depth in either ear, that the worse ear can limit lateralization performance, and that envelope shape changes the effect of AM depth. These results suggest that multiple onsets provided throughout a high-rate amplitude-modulated pulse train can improve lateralization, but only if they are sufficiently large in AM depth and interaurally symmetric.

Both model implementations made characteristic errors associated with envelope type and AM depth; neither model accounted for their interaction. One explanation is that both models overestimated the contributions of ITDs in the stimulus offset (i.e., the last 1–3 pulses of each cycle for the ramped stimuli). This is an important finding since, to our knowledge, no previous modeling efforts have been made to capture the effects of high-rate amplitude-modulated pulse trains. Previous models have accurately predicted the relationship between ITD lateralization and envelope shape for AM applied to tone bursts, including the same Klug implementation used here (Klein-Hennig *et al.*, 2011; Klug *et al.*, 2020). Interestingly, additional models have been used to explain the effects of sharp stimulus onsets or offsets in cells of the inferior colliculus, demonstrating differential effects of excitation and inhibition depending upon the envelope shape (Dietz *et al.*, 2016). It may be that a similar approach is required for high-rate amplitude-modulated pulse trains.

IV. EXPERIMENT 3: INTERACTIONS WITH PLACE-OF-STIMULATION MISMATCH

A. Motivation

The goal of experiment 3 was to explore how interaural spectral asymmetry [i.e., place-of-stimulation mismatch (Cleary *et al.*, 2022)] interacts with interaural temporal asymmetry in lateralization of envelope ITDs. Interaural place-of-stimulation mismatch decreases the number of input fibers from each ear that can be compared to compute an ITD. Decreasing AM depth in one or both ears is thought to introduce less consistent temporal responses of input fibers, simulating interaural temporal asymmetry. Reducing the number of overlapping neurons to compute ITDs by increasing interaural place-of-stimulation mismatch was predicted to interact with interaural temporal asymmetry, leading to the smallest lateralization ranges. It was therefore hypothesized that the effects of interaural temporal asymmetry and place-of-stimulation mismatch might be multiplicative, resulting in a greater decrement when co-occurring than could be explained with either factor alone.

B. Methods

Sixteen new listeners participated in experiment 3 (ages 18–26 years; mean age: 21.6 years). One participant did not provide their age. All participants met the same audiological criteria as in experiment 1, using the same equipment and procedures. The only exception was that the carrier frequency of the Gaussian-enveloped tone was varied such that it resulted in differing degrees of interaural place-of-stimulation mismatch (0, 1.13, 2.25, or 3.38 mm), based on the frequency-to-place map from Greenwood (1990). The resulting center frequencies were 4.00, 4.68, 5.51, and 6.46 kHz, with bandwidths of 1.74, 2.02, 2.37, and 2.77 kHz. As the center frequency increases and the bandwidth increases, the sharpness of the first-order modulator (i.e., the Gaussian envelope) also increases. However, for the range of parameters being tested in the present experiment, there appears to be no effect of Gaussian envelope sharpening on ITD sensitivity in younger listeners with NH (Mayo *et al.*, 2021). The ear and direction of mismatch (by shifting up from 4 kHz or down from 6.5 kHz) was counterbalanced across listeners. Because of the additional number of combinations based on experimental variables, only 50%:50% and 20%:50% AM depth were tested. Testing consisted of 20 repetitions × 9 ITDs × 2 AM depths × 4 mismatches = 1440 trials, and took place over approximately 6 h.

C. Results

1. Behavioral results

Lateralization range is shown in Fig. 5. Based on the literature, we expected lateralization range to be similar whether the opposite ear was shifted up or down in frequency. Thus, for the results shown in Fig. 5(A), results are averaged between groups of listeners. Individual results are shown in Fig. 5(B) and model predictions are shown in Fig. 5(C), separated by the direction in which the opposite ear was shifted in frequency to characterize model behavior. It was hypothesized that lower AM depth and increased place-of-stimulation mismatch would result in reduced lateralization range. There was a significant effect of AM depth [$F(1,105) = 21.626$, $p < 0.0001$] and place-of-stimulation mismatch [$F(3,105) = 32.818$, $p < 0.0001$]. There was not a significant AM depth × interaural place-of-stimulation mismatch interaction [$F(3,105) = 2.209$, $p = 0.091$]. *Post hoc* comparisons revealed that there lateralization range was significantly larger for 0 mm compared to 2.25 mm [$t(105) = 4.239$, $p < 0.001$], 0 mm compared to 3.38 mm [$t(105) = 9.207$, $p < 0.0001$], 1.13 mm compared to 2.25 mm [$t(105) = 2.758$, $p < 0.05$], 1.1 mm compared to 3.38 mm [$t(105) = 7.726$, $p < 0.0001$], and 2.25 mm compared to 3.38 mm [$t(105) = 4.968$, $p < 0.0001$], but not 0 mm compared to 1.13 mm mismatch [$t(105) = 1.481$, $p = 0.452$]. For all but the smallest amounts of interaural place-of-stimulation mismatch, the lateralization range decreased with increasing mismatch.

2. Modeling

The Akeroyd implementation yielded a lower adjusted R^2 than previous experiments (0.743). The Klug implementation performed even worse with an adjusted R^2 of 0.289. No tests of significance to compare these R^2 values to each other or previous values were made. Both models made different errors. The Akeroyd implementation showed an opposite relationship between center frequency and lateralization range [Fig. 5(C)]. The discontinuity in Fig. 5(C) for the Akeroyd implementation was driven by changes in center frequency. When mismatch was simulated by decreasing center frequency, one ear was presented with 6.5 kHz. Thus, this result demonstrates that the Akeroyd implementation

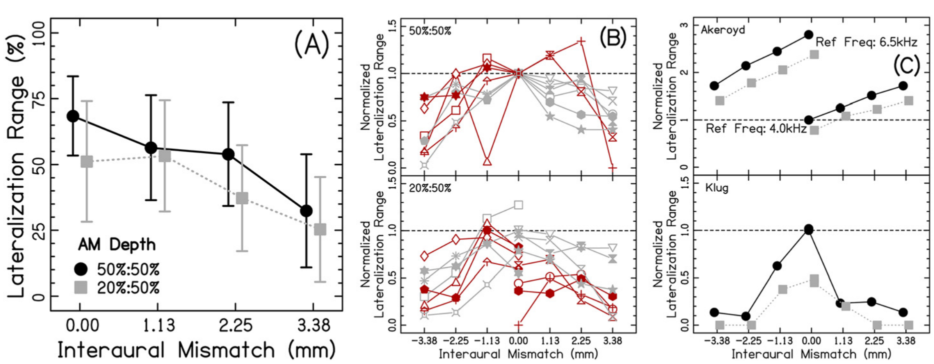

FIG. 5. Lateralization range by interaural place-of-stimulation mismatch and AM depth. The *x* axis corresponds to interaural place-of-stimulation mismatch, and the *y* axis corresponds to the lateralization range. (A) Average data ±1 standard deviation. (B) Individual performance is shown offset in gray or red. Listeners (shown in red) had a lateralization range that was greater than that observed with 0 mm for 1.13, 2.25, or 3.38 mm interaural place-of-stimulation mismatch (contrary to hypotheses). Lateralization ranges were normalized to 0 mm mismatch at 50%:50% AM depth. The top and bottom row show 50%:50% and 20%:50% AM depth, respectively. (C) The top and bottom row show model predictions for the Akeroyd and Klug implementations, respectively. Lateralization ranges were normalized to 0 mm mismatch at 50%:50% AM depth. Negative values for interaural place mismatch indicate that the frequency in the opposite ear was shifted downward from 6.5 kHz. Positive values for interaural mismatch indicate that the frequency in the opposite ear was shifted up from 4.0 kHz.

predicted greater lateralization ranges with higher center frequency. In contrast, the Klug implementation accurately predicted the change in lateralization range with AM depth and interaural place-of-stimulation mismatch [Fig. 5(C)].

D. Discussion

Experiment 3 investigated the impact of interaural place-of-stimulation mismatch and AM depth on envelope ITD lateralization. We hypothesized that there would be an interaction between these factors, with the greatest amounts of interaural place-of-stimulation mismatch and smaller AM depth in one ear yielding the greatest reductions in lateralization range. The results demonstrated no significant interaction, and instead showed that effects of interaural place-of-stimulation mismatch and AM depth on lateralization were additive. Lateralization was extremely poor when interaural place-of-stimulation was greatest and temporal fidelity was reduced in one ear. These findings are consistent with the binaural system having fewer "looks" at noisier envelope ITDs with interaural place-of-stimulation mismatch and poor temporal fidelity in one or both ears (e.g., "readout" window) (Stecker, 2018). Critically, when interaural place-of-stimulation mismatch and reduced temporal fidelity co-occur, lateralization ranges decreased below the level of performance observed when stimuli were matched in place-of-stimulation, but above when AM depth was 0% (i.e., pulses were of constant amplitude; see Appendix). Thus, place-of-stimulation may be the more greatly limiting factor, since envelope ITDs from disparate places-of-stimulation may not be useful for lateralization (Goupell *et al.*, 2013b; Kan *et al.*, 2013; Kan *et al.*, 2015; Kan *et al.*, 2019).

Previous experiments investigating interaural place-of-stimulation mismatch have focused primarily on constant-amplitude pulse trains (i.e., the first-order modulator) (Goupell *et al.*, 2013b; Kan *et al.*, 2013; Kan *et al.*, 2015; Kan *et al.*, 2019) and SAM tones (Blanks *et al.*, 2007; Blanks *et al.*, 2008; Henning, 1974; Nuetzel and Hafter, 1981). The present study was the first study on interaural place-of-stimulation mismatch to investigate high-rate amplitude-modulated pulse trains. Our results are consistent with those from previous studies, suggesting that the utility of ITDs decreases with increasing mismatch. This suggests that the effects of temporal and spectral mismatches were additive rather than interacting.

The largest discrepancy between models and poorest model performance occurred in experiment 3. Both model implementations predicted the effects of interaural place-of-stimulation mismatch for lateralization to a lesser extent than the other effects in experiments 1 and 2. Relative to the largest lateralization range achieved with 0 mm mismatch and 50%:50% AM depth, behavioral results indicated that normalized lateralization range was 0.47 with 50%:50% AM depth and 0.37 with 20%:50% AM depth. The Akeroyd implementation showed consistently monotonic relationships with ITDs, but the change in range of predicted lateralization was incorrect. When 6.7 kHz was presented to both ears, predicted lateralization was largest (2.8 times higher than when 4 kHz was presented to both ears). The Akeroyd implementation predicted larger lateralization ranges for higher frequencies [Fig. 5(C)], which was surprising given that a similar model predicted poorer ITD just-noticeable-differences for higher (6 and 10 kHz) compared to lower (4 kHz) center frequency trains of constant-amplitude transients (Bernstein and Trahiotis, 2002, 2014).[2] Lateralization studies did not evaluate effects of center frequency. When the Akeroyd implementation was tested with 4 vs 6 kHz SAM tones (data not shown), it also resulted in larger predicted lateralization range for higher frequencies. The Klug implementation showed highly non-monotonic predictions for ITD lateralization when stimuli had non-zero interaural place-of-stimulation mismatch (see the supplementary material). Despite the non-monotonic trends in predicted lateralization across ITDs, the Klug implementation predicted trends in lateralization range. These trends were exaggerated (at the interaural place-of-stimulation mismatch of 3.38 mm, normalized lateralization range of 0.13 for 50%:50% AM depth and 0.00 for 20%:50% AM depth were predicted) relative to behavioral results. It is worth noting that effect of interaural place-of-stimulation mismatch is consistent with modeling of auditory brainstem responses using the same underlying LSO model as the Klug implementation (Brown *et al.*, 2019). Despite the Akeroyd implementation's estimated effect of interaural place-of-stimulation mismatch, both models correctly predicted the additive effects of asymmetric AM depth [Fig. 5(C)], suggesting that poorer lateralization with interaural frequency and temporal mismatch may indeed result from fewer overlapping neurons to the noisy temporal inputs used to calculate the ITD.

V. GENERAL DISCUSSION

A. Interaural asymmetries in temporal encoding

The experiments in the present manuscript investigated the relationship between interaural temporal asymmetry with two factors known to influence ITD lateralization: envelope shape and interaural spectral asymmetry (i.e., place-of-stimulation mismatch). Recent studies in listeners with BiCIs show that when they have one ear that was left unstimulated for long periods of time, have poorer speech understanding (e.g., Blamey *et al.*, 2012; Goupell *et al.*, 2018), poorer localization performance (Reeder *et al.*, 2014), and poorer sensitivity to binaural cues (Thakkar *et al.*, 2020). Large differences between the ears have been related to poor and/or abnormal speech understanding when target speech is in the poorer ear (Goupell *et al.*, 2016; Goupell *et al.*, 2018; Mosnier *et al.*, 2009). Together, these and other studies (Anderson *et al.*, 2019b; Anderson *et al.*, 2022; Ihlefeld *et al.*, 2015) suggest that the poorer ear limits binaural outcomes. The present results replicated previous findings and expanded them by evaluating a larger range of stimulus parameters (i.e., envelope shape and place-of-stimulation mismatch) using pulsatile stimulation.

Recent evidence implies that interaural asymmetries limit binaural outcomes; however, many of the conceptual and computational models associated with binaural processing have assumed interaural symmetry. The present experiment demonstrates some ways that different kinds of interaural asymmetry can interact with other factors that affect envelope ITD lateralization and contribute to variability in performance that is not currently addressed in the literature. Modeling results will be discussed further in Sec. V C.

B. Description of results and the relevance to listeners with CIs

The present experiment simulated interaural asymmetry in temporal representations by manipulating the AM depth of a second-order modulator. Using sinusoidal (Figs. 3 and 5) and triangular envelope shapes (Fig. 4) on trains of Gaussian-enveloped tones, results further showed that lateralization range decreased when at least one ear had reduced AM depth, except when lateralization was already small (e.g., for ramped envelope shapes in Fig. 4 and large interaural place-of-stimulation mismatch in Fig. 5). Reducing AM depth was meant to simulate poorer phase locking (Fig. 2) due to changes in the auditory periphery for listeners with BiCIs (Fig. 1). Small AM depth is analogous to reduced dynamic range at the level of the auditory nerve. Dynamic range as measured at the level of CI programming software is one psychophysical predictor for the ENI for listeners (Bierer, 2010; Long *et al.*, 2014). However, the "true" dynamic range of the auditory nerve (e.g., the relationship between input current to the neuron and spike rate) is not known for patients. Both increased distance of CI electrodes from the auditory nerve and peripheral deterioration are suspected to affect the dynamic range of auditory nerve fibers as measured at the level of CI programming software (Bierer, 2010; Goldwyn *et al.*, 2010; Schvartz-Leyzac *et al.*, 2020). Binaural masking level difference and ITD discrimination thresholds both improve with increasing dynamic range (Todd *et al.*, 2017). Similarly, increased AM depth for SAM pulse trains results in greater ITD sensitivity in listeners with BiCIs (Ihlefeld *et al.*, 2014). Thus, one implication of the results from the present study is that reduced dynamic range limits binaural processing.

Previous studies of envelope shape have demonstrated differences between listeners with NH and BiCIs. In particular, listeners with NH seem to be sensitive to the attack time of AM (Bernstein and Trahiotis, 2002, 2009, 2011; Dietz *et al.*, 2015; Klein-Hennig *et al.*, 2011; Laback *et al.*, 2011), where listeners with BiCIs show no difference between sharp and shallower attack times for monaural (Landsberger, 2008) or binaural tasks (Laback *et al.*, 2011). One important confound between previous BiCI and NH studies was that listeners with BiCIs were presented with amplitude-modulated pulse trains (i.e., their stimuli had pulsatile carriers), where listeners with NH were presented with stimuli that had tonal carriers. This sparse sampling of the envelope may have played a role in the lack of effect of envelope shape on BiCI performance. Figure 6 shows the lateralization ranges of listeners that participated in the present experiment with a

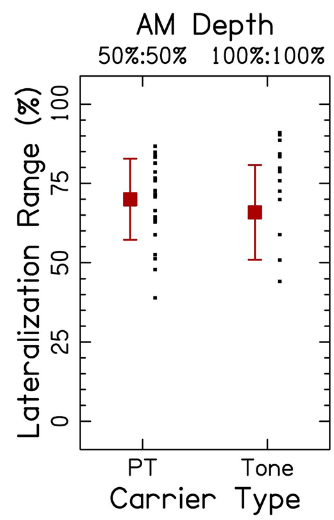

FIG. 6. Lateralization range by carrier type and AM depth. The *x* axis corresponds to the carrier, either a pulse train (PT) or 4 kHz sine tone, as well as the AM depth. The *y* axis corresponds to the lateralization range. Data for SAM tones with 100%:100% AM depth reprinted from Anderson *et al.* (2019a) with permission.

500 pps acoustic pulse train carrier compared to previously published data with SAM tones (Anderson *et al.*, 2019a). Both studies used 100 Hz AM rates and similar lateralization measurement methods. The present study used 50% AM depth in both ears whereas Anderson *et al.*, (2019a) used 100% AM depth. The data show extraordinarily similar distributions and no difference between groups according to a independent two-sample two-tailed *t*-test [$t(36) = 0.338$, $p = 0.971$]. Previously published data using interaurally symmetric SAM tones suggest that reducing AM depth from 100% to 50% would lead to a considerable reduction in lateralization range (Bernstein and Trahiotis, 2011). Our results therefore imply that lateralization of modulated pulse trains either saturates at 50% and higher AM depth, or that pulsatile stimulation improved lateralization of ITDs relative to SAM tones, consistent with Bernstein and Trahiotis (2011) using constant-amplitude pulse trains.

Two additional results from the present study shed important light on this confound between NH and BiCI studies. First, by manipulating the depth of the second-order modulator, lateralization range decreased for listeners with NH in all three experiments. Reducing AM depth also decreased the slope. Second, listeners with NH had greater lateralization range for stimuli with a sharp attack in both ears, but only when AM depth was large. Together, these results imply that pulsatile stimulation is not sufficient to explain differences between listeners with BiCIs and NH. Thus, these differences may have to do with the high degree of phase locking characteristic of electrical stimulation (Dynes and Delgutte, 1992; Javel and Shepherd, 2000), the older average age of listeners in studies with BiCIs compared to NH (Anderson *et al.*, 2019a; Baumgärtel *et al.*, 2017), the nature of listeners' hearing loss, or a combination of all of these factors.

For SAM pulse trains, listeners with NH and BiCIs show different lateralization of ITDs conveyed in different portions of the stimulus (Hu *et al.*, 2017). While listeners with NH heavily weight the onset of high-rate SAM pulse trains, listeners with BiCIs may weight the peak more heavily (Hu *et al.*, 2017). Interestingly, listeners with NH and BiCIs show very similar relationships between rate of sinusoidal AM and lateralization range, with 100 Hz yielding the largest lateralization range, which could be attributed to the slope of AM (Anderson *et al.*, 2019a). Because Hu *et al.* (2017) used very low AM rates (2 or 8 Hz), it remains to be determined whether multiple onsets in high-rate amplitude-modulated pulse trains are similarly useful for listeners with BiCIs.

The amount of interaural place-of-stimulation mismatch used in experiment 3 was within the range that is typically fused into a single spatial percept by listeners with NH (Goupell *et al.*, 2013b; Kan *et al.*, 2019). Anecdotal reports and behavioral responses generally supported the interpretation that listeners perceived one sound image. However, we did not assess the number and width of the sound images perceived in these studies. If interaural decorrelation at the brainstem did indeed increase, this may be a promising area of future research.

C. Assumptions of symmetry in binaural models

In the present experiment, we compared the performance of two highly relevant models of binaural processing. The Akeroyd implementation predicts lateralization based upon frequency- and delay-weighted cross correlation, similar to the type of processing thought to be completed in the MSO. The model utilized by Klug *et al.* (2020) has also been used to predict cellular output of the LSO (Ashida *et al.*, 2016). Thus, both models are reflective of the types of processing that occur in the brainstem to code for envelope ITDs. Moreover, similar models have demonstrated highly accurate predictions of lateralization of constant-amplitude trains of high-frequency modulated stimuli in previous studies (Bernstein and Trahiotis, 2012; Klug *et al.*, 2020).

The findings in the present paper indicate that both the Akeroyd and Klug implementations were predictive of behavioral performance with these novel stimuli. The adjusted R^2 value for each experiment and model implementation is summarized in Table II. Both model implementations had different strengths, particularly in cases of interaural place-of-stimulation mismatch (experiment 3). That is, while the Akeroyd implementation tended to better predict mean lateralization performance across listeners (see supplementary materials for additional details), the Klug implementation tended to demonstrate trends in lateralization ranges more closely corresponding to relative changes in performance (Figs. 3–5). Both models made erroneous predictions related to AM depth and envelope shape. For example, both models predicted greater lateralization ranges than were observed for 20%:50% compared to 20%:20% AM depth, but captured some reduction in lateralization range relative to 50%:50% AM depth (Figs. 3–5).

TABLE II. Adjusted R^2 values for each model implementation by experiment.

	Adjusted R^2	
	Akeroyd implementation	Klug implementation
Experiment 1	0.949	0.786
Experiment 2	0.885	0.743
Experiment 3	0.743	0.289

Both models include coincidence detection as central to their function. If coincidence detection itself leads to the conclusion that interaurally asymmetric AM depth should result in better lateralization than interaurally symmetric, small AM depth, this would have interesting implications for binaural processing. Auditory nerve modeling in Fig. 2 using the stimuli employed in the present study and in the original study (Zilany *et al.*, 2014), as well as extracellular recordings from the cat (Joris and Yin, 1992), show that phase locking decreases with decreasing AM depth. In the realm of probability, this could be expressed as greater spread or variance associated with a probability distribution. A simple model of the probability of coincidence within a given time window for the left and right channel and monaurally symmetric over time is given in Eq. (3), similar to the classical normalized cross correlation function

$$P(C) = \int_{t_1}^{t_2} f_L(x) f_R(x)\, dx, \qquad (3)$$

where $P(C)$ is the probability of coincident spikes from the frequency-matched left and right channel (i.e., the joint probability of f_L and f_R) within the time window $[t_1, t_2]$, $f_L(x)$ and $f_R(x)$ are probability density functions that are continuously defined within $[t_1, t_2]$ for the left and right channel, and x is time. A lower AM depth in both ears increases the spread of the probability density functions f_L and f_R, which results in a decrease in $P(C)$ for many possible values of $[t_1, t_2]$. A decrease in $P(C)$ is supported by predictions of poorer ITD sensitivity with lower and symmetric AM depth using coincidence-based models, results which were replicated for the stimuli and coincidence-based models in the present study (Figs. 3–5). If, instead, the AM depth is reduced in only the left ear and $f_R \geq f_L$ between $[t_1, t_2]$, this guarantees that $P(C)$ is greater than when the AM depth is lower in both ears. Even if this is not guaranteed, it is likely that lower AM depth in one ear would lead to an increase in $P(C)$ compared to lower symmetric AM depths, especially for $[t_1, t_2]$ centered around the peaks of f_L and f_R where $P(C)$ is greatest. This conclusion is supported by the predictions from both models in experiments 1 and 2 in the present study. It is difficult to generalize these findings to experiment 3 because of the added complication of interaural place-of-stimulation mismatch.

The simple model [Eq. (3)] suggests that a purely coincidence-detection-based model of binaural processing is likely to predict that interaurally asymmetric phase locking

https://doi.org/10.1121/10.0039519 JASA

results in better binaural sensitivity than poor symmetric phase locking. However, the results from all experiments in the present study and another study with patients who use BiCIs (Ihlefeld *et al.*, 2015) do not support this conclusion. This implies that coincidence detection is either not the only mechanism involved in computing ITDs, or that the system is more dynamic. A more complex relationship between left and right inputs than pure coincidence detection fits the recent view that binaural processing neurons in the brainstem do not act as time-invariant input-output functions, but instead represent a dynamic system that adapts to the statistics of stimuli (Gleiss *et al.*, 2019). In the present study, when asymmetric AM depth was applied, the mean level was maintained, introducing differences between the peak and trough of each cycle. Thus, the ILD was varied over time. Time-varying binaural cues have been associated with a spatially diffuse sound image (a possible precursor to a lack of fusion) (Whitmer *et al.*, 2014) and are speculated to play a role in poorer ITD sensitivity of listeners with BiCIs (Anderson *et al.*, 2019a; Goupell, 2015; Goupell and Litovsky, 2015). Thus, adaptation to stimulus statistics could be central to binaural perception, which could help explain the present difference between models and behavioral data. This effect is still assumed to be driven in part by phase locking between the left- and right-ear inputs to binaural neurons.

D. Limitations and future directions

The present study had several limitations. While across-group trends (e.g., effects of pulse rate on lateralization of constant-amplitude pulse trains) were consistent with previous studies (Bernstein and Trahiotis, 2014; Monaghan *et al.*, 2015), the sample sizes used here were relatively small, especially when considering the variability across listeners (see supplementary material for additional details including individual lateralization curves). Variability in performance is commonly observed in lateralization tasks using the same procedure as that used in the present experiment, even in the presence of normal and symmetric hearing thresholds (Goupell *et al.*, 2021). Most results presented here are consistent with previously published experiments in listeners with NH and were discussed in more detail in the discussion section following each experiment.

It is difficult to generalize the results from the present experiment directly to listeners with BiCIs. Electrical stimulation via a CI results in highly synchronous auditory nerve firing in cats (Dynes and Delgutte, 1992; Javel and Shepherd, 2000), although this has not been confirmed in humans. It is unclear whether limitations to temporal encoding occur at the level of individual or population of nerve fibers in patients with BiCIs. We chose to simulate poorer temporal fidelity by reducing AM depth (to simulate a reduced dynamic range for listeners with CIs). Even if our manipulation is not representative of changes in temporal representations due to phase locking of the auditory nerve, the findings are in agreement with studies in listeners with BiCIs showing reduced binaural sensitivity at lower AM depths (Ihlefeld *et al.*, 2014) and smaller dynamic range in current levels at each electrode (Todd *et al.*, 2017). Furthermore, the listeners in the present study were much younger on average than those tested in studies of listeners with BiCIs and aging is associated with reduced lateralization ranges (Anderson *et al.*, 2019a; Baumgärtel *et al.*, 2017). Since aging and hearing loss interact to produce poorer binaural temporal sensitivity (Anderson *et al.*, 2019a; Baumgärtel *et al.*, 2017), testing older NH listeners and younger BiCI listeners is an important next step.

The ITDs conveyed by BiCIs have inconsistent ITDs between the temporal fine structure (i.e., electrical pulses) and envelope (Dennison *et al.*, 2022; Gray *et al.*, 2021). In contrast, the present study used whole-waveform ITDs (ITDs in the carrier pulses and envelope ITDs were congruent). An alternative approach would have been to jitter ITDs in the pulse train, or fix the ITD of the constant-amplitude pulse train at 0 μs and only apply an ITD to the envelope. In order to attain a high pulse rate with 3 mm bandwidth acoustic pulse trains, there was very little pause time between pulses. It was therefore not possible to jitter ITDs with 500 pps acoustic pulse trains, so we prioritized using as high a pulse rate as possible. Fixing ITDs of the constant-amplitude pulse train at 0 μs may have artificially biased lateralization toward the center of the head and it would not be any more ecologically valid than conveying coherent ITDs in the temporal fine structure. From Fig. 7 in the Appendix, listeners were still able to use ITDs from the pulsatile carrier to complete lateralization and attain a lateralization range of approximately 40%. Thus, our approach of applying whole-waveform ITDs represents a scenario for BiCI output where both envelope and temporal fine-structure ITDs are presented.

Stimuli in the present experiment simulated single-channel stimulation with a CI, which is not generalizable to actual CI listening. With multi-channel monopolar stimulation, spectro-temporal smearing via channel interaction

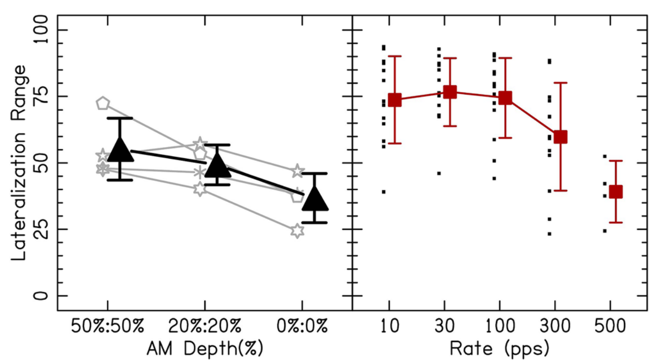

FIG. 7. Lateralization range by (A) AM depth, (B) pulse rate. The y axis corresponds to the extent of lateralization, with mean $\pm$ 1 standard deviation shown by each point. (A) The x axis corresponds to the AM depth, (B) the x axis corresponds to the pulse rate for acoustic pulse trains. Data from pulse rates of 10–300 pps are reprinted with permission from Anderson *et al.*, J. Acoust. Soc. Am. **146**(2), 1189–1206 (2019a). Copyright 2019 Acoustical Society of America.

would occur (e.g., Bierer, 2010), further distorting the envelope and the ability to compute ITDs (e.g., Kan *et al.*, 2019; Lindenbeck *et al.*, 2024).

The pulse rates used in the present study were lower than the clinical standard for listeners using most contemporary CI processors, which use pulse rates of about 1000–4000 pps per channel. Most CI processing strategies do not preserve temporal fine structure, so ITDs are primarily available from the temporal envelope (Gray *et al.*, 2021). To date, there is relatively less research at higher rates near 500–1000 pps compared to lower rates near 100 pps. This may have to do with the upper-limit of pulses that can be represented without temporal overlap (Goupell *et al.*, 2013b). That is, we chose to use 500 pps because that was near the maximum number of pulses with 3 mm bandwidth that could be presented without resulting in substantive temporal overlap between each pulse.

E. Summary and conclusions

Based on the data in this study, several conclusions can be drawn with respect to lateralization of envelope ITDs under conditions of interaural asymmetry:

(1) Lateralization range associated with envelope ITDs was significantly smaller when one (asymmetric) or both (symmetric) ears had a smaller AM depth (20% compared to 50%) (Figs. 3–5), where AM depth was used to simulate reduced temporal fidelity.
(2) Lateralization of high-rate amplitude-modulated pulse trains was facilitated by interaurally symmetric sharp temporal onsets and inhibited by sloping temporal onsets, in the temporal envelope (Fig. 4). This finding is consistent with weighting of the onset for high-rate amplitude-modulated pulse trains in listeners with NH (Hu *et al.*, 2017; Stecker, 2018).
(3) Reduced lateralization from increasing interaural place-of-stimulation mismatch and reduced AM depth were additive (Fig. 5).
(4) EE-based cross correlation and EI-based models of binaural processing predicted lateralization of envelope ITDs for interaurally symmetric AM depths (20% and 50%), but slightly overestimated lateralization range for interaurally asymmetric AM depths (Figs. 3–5). In other words, they captured some of the effect of interaurally asymmetric AM depth. A simple model of pure coincidence detection replicates overestimation of lateralization of asymmetric AM depths (Eq. 3), implying that an additional mechanism besides coincidence detection is involved in ITD lateralization with interaurally asymmetric AM depth.
(5) EE-based cross correlation and EI-based models of binaural processing did not accurately predict effects of second-order envelope shape for high-rate amplitude-modulated pulse trains (Fig. 4). The models predicted similar performance for pulse trains with second-order AM and a temporally sharp onset or offset. Previous studies using amplitude-modulated tones with sharp temporal onsets suggested increased sensitivity to ITDs with sharp onsets (e.g., Dietz *et al.*, 2015; Klein-Hennig *et al.*, 2011).
(6) EE-based cross correlation and EI-based models of binaural processing poorly predicted effects of interaural place-of-stimulation mismatch [Fig. 5(C)]. The EE-based model predicted monotonic relationships between ITDs and lateralization, but increasing lateralization range with increasing average center frequency. The EI-based model accurately predicted changes in lateralization range (decreased lateralization range with increasing frequency mismatch and decreasing AM depth in one ear) but demonstrated highly non-monotonic relationships between ITDs and lateralization with interaural frequency mismatch.

SUPPLEMENTARY MATERIAL

See the supplementary material for supplementary figures, additional appendixes, and all data and code used for analysis.

ACKNOWLEDGEMENTS

The authors would like to thank Dr. Mathias Dietz for his thoughtful contributions as this project developed, and particularly for his mentorship in modeling for S.R.A. Portions of this work appear in the dissertation of S.R.A. (Anderson, 2022) and were presented at the 2021 Association for Research in Otolaryngology MidWinter meeting online. This work was supported by Grant Nos. F31 DC018483-01A1 awarded to S.R.A., R01 DC020316 awarded to M.J.G., R03 DC015321 awarded to A.K., R01 DC003083 and R01 DC020355 awarded to R.Y.L., and NIH-NICHD U54HD090256 awarded to the Waisman Center.

AUTHOR DECLARATIONS
Conflict of Interest

At the time this work was submitted for publication, S.R.A. was employed by Cochlear Ltd.

DATA AVAILABILITY

All data and code used for analysis are included in the supplementary material.

[1]The code for the Akeroyd implementation is available from http://doi.org/10.17639/nott.320.

[2]Most behavioral and modeling studies of center frequency have focused on ITD sensitivity. One study has explored the effects of high center frequencies on lateralization of envelope ITDs (Rule, 1994). They used a 200-Hz sinusoidal AM with center frequencies of 2.2-, 3.2-, 4.2-, and 5.2-kHz carriers and 100% AM depth, showing a slight decrease in lateralization range computed at $\pm 600\ \mu s$ and averaged across listeners.

APPENDIX

It was important to characterize the lateralization range for stimuli that were unmodulated to confirm the usefulness of cues in the pulses compared to the envelope (i.e., first- compared to second-order modulations) contributed to lateralization. Note that the pulse rate used in the present experiment was higher than that used in previous NH experiments and lower than that typical of CI stimulation. Much previous research has been dedicated to the "rate limitation" to binaural processing in listeners with NH (for review, see Stecker *et al.*, 2021) and BiCIs (for review, see Kan and Litovsky, 2015; Laback *et al.*, 2015). Most of this research agrees with the consensus that the rate limitation is somewhere near 300 pps, meaning that sensitivity to ITDs decreases precipitously above 300 pps. However, some listeners with NH maintain sensitivity to ITDs in constant-amplitude stimuli at pulse rates of ~900 Hz (e.g., Bernstein and Trahiotis, 2014; Monaghan *et al.*, 2015). Thus, we tested a small group of listeners with NH using 50%:50%, 20%:20%, and 0%:0% AM depth to determine whether the lateralization range would decrease if stimuli were constant amplitude (i.e., if AM depth was further reduced to 0%:0%).

We included ITDs of 0, ±100, ±200, ±400, ±800, ±1200, and ±1600 μs. The ±1200 and ±1600 μs ITDs would result in an interaural phase difference greater than π for the pulsatile carrier but less than π for the sinusoidal AM. If listeners attended to the pulsatile carrier rather than the envelope, then the perceived intracranial location should move back toward the center of the head for ±1200 and ±1600 μs. If listeners attended to the envelope, onset, or offset, then the magnitude of lateralization should be equal or greater than the maximum magnitude of lateralization for ±1200 and ±1600 μs. Lateralization range was assessed as the absolute difference in lateralization values from the fitted curves at ±1000 μs.

Four listeners (ages 19–29 years; mean age: 21.5 years) met the same audiological criteria as the experiments and the same equipment and procedures were used. Twenty repetitions per ITD were collected except for listener TZA, who only completed ten repetitions per ITD for the 50%:50% and 0%:0% AM depth conditions because of time limitations. This resulted in 20 repetitions × 11 ITDs × 3 AM depths = 660 trials, which took approximately 1.5 h to collect.

Lateralization ranges for differing AM depths are presented in Fig. 7(A). They show that lateralization range decreased slightly on average between 20%:20% and 0%:0% AM depth. This effect was driven by three of four listeners. The lateralization ranges in Fig. 7(B) were all computed for ±1000 μs ITDs to be consistent with the previous manuscript, in contrast to the rest of the present manuscript where they were computed at ±800 μs (Anderson *et al.*, 2019a). The data for 500 pps are from the listeners in the present experiment and demonstrate a consistent trend with the previously published data. This trend is in agreement with studies of ITD sensitivity using high-rate high-frequency trains of transients (Bernstein and Trahiotis, 2014; Monaghan *et al.*, 2015).

The results presented in this appendix suggest two important conclusions about how listeners completed the lateralization experiment. First, perceived lateralization of ±1200 and ±1600 continued to be of large magnitude and was not toward the center of the head, which suggests that listeners relied on the onset, offset, or ongoing temporal envelope (i.e., second-order AM) of the sound for lateralization rather than ongoing ITDs in the pulse train. Results from the 0%:0% AM depth (i.e., constant-amplitude) in particular suggest that listeners may have been able to resolve interaural phase ambiguity using the ITDs at the onset and offset of stimuli. Second, these results demonstrate that 20%:20% AM depth was able to be lateralized to a greater extent than 0%:0% AM depth.

Akeroyd, M. A. (**2003**). "Threshold differences for interaural time delays carried by double vowels," J. Acoust. Soc. Am. **114**(4), 2167–2177.

Anderson, S. R. (**2022**). "Mechanisms that underlie poorer binaural outcomes in patients with asymmetrical hearing and bilateral cochlear implants," Ph.D. dissertation, University of Wisconsin-Madison, Madison, WI.

Anderson, S. R., Burg, E., Suveg, L., and Litovsky, R. Y. (**2024**). "Review of binaural processing with asymmetrical hearing outcomes in patients with bilateral cochlear implants," Trends Hear. **28**, 1–25.

Anderson, S. R., Easter, K., and Goupell, M. J. (**2019a**). "Effects of rate and age in processing interaural time and level differences in normal-hearing and bilateral cochlear-implant listeners," J. Acoust. Soc. Am. **146**(5), 3232–3254.

Anderson, S. R., Gallun, F. J., and Litovsky, R. Y. (**2023**). "Interaural asymmetry of dynamic range: Abnormal fusion, bilateral interference, and shifts in attention," Front. Neurosci. **16**(January), 1018190.

Anderson, S. R., Kan, A., and Litovsky, R. Y. (**2019b**). "Asymmetric temporal envelope encoding: Implications for within- and across-ear envelope comparison," J. Acoust. Soc. Am. **146**(2), 1189–1206.

Anderson, S. R., Kan, A., and Litovsky, R. Y. (**2022**). "Asymmetric temporal envelope sensitivity: Within- and across-ear envelope comparisons in listeners with bilateral cochlear implants," J. Acoust. Soc. Am. **152**(6), 3294–3312.

Aronoff, J. M., Yoon, Y., Freed, D. J., Vermiglio, A. J., Pal, I., and Soli, S. D. (**2010**). "The use of interaural time and level difference cues by bilateral cochlear implant users," J. Acoust. Soc. Am. **127**(3), EL87–EL92.

Ashida, G., Kretzberg, J., and Tollin, D. J. (**2016**). "Roles for coincidence detection in coding amplitude-modulated sounds," PLoS Comput. Biol. **12**(6), e1004997.

Bates, D., Machler, M., Bolker, B., and Walker, S. (**2015**). "Fitting linear mixed-effects models using lme4," J. Stat. Softw. **67**(1), 1–48.

Baumgärtel, R. M., Hu, H., Kollmeier, B., and Dietz, M. (**2017**). "Extent of lateralization at large interaural time differences in simulated electric hearing and bilateral cochlear implant users," J. Acoust. Soc. Am. **141**(4), 2338–2352.

Bernstein, L. R., and Trahiotis, C. (**2002**). "Enhancing sensitivity to interaural delays at high frequencies by using 'transposed stimuli,'" J. Acoust. Soc. Am. **112**(3), 1026–1036.

Bernstein, L. R., and Trahiotis, C. (**2009**). "How sensitivity to ongoing interaural temporal disparities is affected by manipulations of temporal features of the envelopes of high-frequency stimuli," J. Acoust. Soc. Am. **125**(5), 3234–3242.

Bernstein, L. R., and Trahiotis, C. (**2011**). "Lateralization produced by envelope-based interaural temporal disparities of high-frequency, raised-sine stimuli: Empirical data and modeling," J. Acoust. Soc. Am. **129**(3), 1501–1508.

Bernstein, L. R., and Trahiotis, C. (**2012**). "Lateralization produced by interaural temporal and intensitive disparities of high-frequency, raised-sine stimuli: Data and modeling," J. Acoust. Soc. Am. **131**(1), 409–415.

Bernstein, L. R., and Trahiotis, C. (**2014**). "Sensitivity to envelope-based interaural delays at high frequencies: Center frequency affects the envelope rate-limitation," J. Acoust. Soc. Am. **135**(2), 808–816.

Best, V., Baumgartner, R., Lavandier, M., Majdak, P., and Kopčo, N. (**2020**). "Sound externalization: A review of recent research," Trends Hear. **24**, 1–14.

Bierer, J. A. (**2010**). "Probing the electrode-neuron interface with focused cochlear implant stimulation," Trends Amplif. **14**(2), 84–95.

Bierer, J. A., and Nye, A. D. (**2014**). "Comparisons between detection threshold and loudness perception for individual cochlear implant channels," Ear Hear. **35**(6), 641–651.

Blamey, P., Artieres, F., Başkent, D., Bergeron, F., Beynon, A., Burke, E., Norbert Dillier, N., Dowell, R., Fraysse, B., Gallégo, S., Govaerts, P. J., Green, K., Huber, A. M., Kleine-Punte, A., Maat, B., Marx, M., Mawman, D., Mosnier, I., O'Connor, A. F., O'Leary, S., Rousset, A., Schauwers, K., Skarzynski, H., Skarzynski, P. H., Sterkers, O., Terranti, A., Truy, E., Van de Heyning, P., Venail, F., Vincent, D., and Lazard, D. S. (**2012**). "Factors affecting auditory performance of postlinguistically deaf adults using cochlear implants: An update with 2251 patients," Audiol. Neurotol. **18**(1), 36–47.

Blanks, D. A., Buss, E., Grose, J. H., Fitzpatrick, D. C., and Hall, J. W., III (**2008**). "Interaural time discrimination of envelopes carried on high-frequency tones as a function of level and interaural carrier mismatch," Ear Hear. **29**(5), 674–683.

Blanks, D. A., Roberts, J. M., Buss, E., Hall, J. W., and Fitzpatrick, D. C. (**2007**). "Neural and behavioral sensitivity to interaural time differences using amplitude modulated tones with mismatched carrier frequencies," J. Assoc. Res. Otolarygol. **8**(3), 393–408.

Boudreau, J. C., and Titani, C. (**1968**). "Binaural interaction in the cat superior olive S segment," J. Neurophysiol. **31**(3), 442–454.

Brand, A., Behrend, O., Marquardt, T., McAlpine, D., and Grothe, B. (**2002**). "Precise inhibition is essential for microsecond interaural time difference coding," Nature **417**(6888), 543–547.

Bronkhorst, A. W., and Plomp, R. (**1988**). "The effect of head-induced interaural time and level differences on speech intelligibility in noise," J. Acoust. Soc. Am. **83**(4), 1508–1516.

Brown, A. D., Anbuhl, K. L., Gilmer, J. I., and Tollin, D. J. (**2019**). "Between-ear sound frequency disparity modulates a brain stem biomarker of binaural hearing," J. Neurophysiol. **122**(3), 1110–1122.

Brown, A. D., and Tollin, D. J. (**2016**). "Slow temporal integration enables robust neural coding and perception of a cue to sound source location," J. Neurosci. **36**(38), 9908–9921.

Bruce, I. C., Erfani, Y., and Zilany, M. S. A. (**2018**). "A phenomenological model of the synapse between the inner hair cell and auditory nerve: Implications of limited neurotransmitter release sites," Hear. Res. **360**, 40–54.

Buchholz, J. M., Le Goff, N., and Dau, T. (**2018**). "Localization of broadband sounds carrying interaural time differences: Effects of frequency, reference location, and interaural coherence," J. Acoust. Soc. Am. **144**(4), 2225–2237.

Cleary, M., Bernstein, J. G. W., Stakhovskaya, O. A., Noble, J., Kolberg, E., Jensen, K. K., Hoa, M., Kim, H. J., and Goupell, M. J. (**2022**). "The relationship between interaural insertion-depth differences, scalar location, and interaural time-difference processing in adult bilateral cochlear-implant listeners," Trends Hear. **26**, 1–24.

Dennison, S. R., Jones, H. G., Kan, A., and Litovsky, R. Y. (**2022**). "The impact of synchronized cochlear implant sampling and stimulation on free-field spatial hearing outcomes: Comparing the ciPDA research processor to clinical processors," Ear Hear. **43**(4), 1262–1272.

Dietz, M. (**2016**). "Models of the electrically stimulated binaural system: A review," Netw. Comput. Neural Syst. **27**(2–3), 186–211.

Dietz, M., Klein-Hennig, M., and Hohmann, V. (**2015**). "The influence of pause, attack, and decay duration of the ongoing envelope on sound lateralization," J. Acoust. Soc. Am. **137**(2), EL137–EL143.

Dietz, M., Wang, L., Greenberg, D., and McAlpine, D. (**2016**). "Sensitivity to interaural time differences conveyed in the stimulus envelope: Estimating inputs of binaural neurons through the temporal analysis of spike trains," J. Assoc. Res. Otolarygol. **17**(4), 313–330.

Dynes, S. B. C., and Delgutte, B. (**1992**). "Phase-locking of auditory-nerve discharges to sinusoidal electric stimulation of the cochlea," Hear. Res. **58**, 79–90.

Fischer, T., Schmid, C., Kompis, M., Mantokoudis, G., Caversaccio, M., and Wimmer, W. (**2021**). "Effects of temporal fine structure preservation on spatial hearing in bilateral cochlear implant users," J. Acoust. Soc. Am. **150**(2), 673–686.

Fitzgerald, M. B., Kan, A., and Goupell, M. J. (**2015**). "Bilateral loudness balancing and distorted spatial perception in recipients of bilateral cochlear implants," Ear Hear. **36**(5), e225–e236.

Franken, T. P., Joris, P. X., and Smith, P. H. (**2018**). "Principal cells of the brainstem's interaural sound level detector are temporal differentiators rather than integrators," eLife **7**(e33854), 1–25.

Fu, Q. J. (**2005**). "Loudness growth in cochlear implants: Effect of stimulation rate and electrode configuration," Hear. Res. **202**, 55–62.

Gleiss, H., Encke, J., Lingner, A., Jennings, T. R., Brosel, S., Kunz, L., Grothe, B., and Pecka, M. (**2019**). "Cooperative population coding facilitates efficient sound-source separability by adaptation to input statistics," PLoS Biol. **17**(7), e3000150–24.

Goldberg, J. M., and Brown, P. B. (**1969**). "Response of binaural neurons of dog superior olivary complex to dichotic tonal stimuli: Some physiological mechanisms of sound localization," J. Neurophysiol. **32**(4), 613–636.

Golding, N. L., and Oertel, D. (**2012**). "Synaptic integration in dendrites: Exceptional need for speed," J. Physiol. **590**(22), 5563–5569.

Goldwyn, J. H., Bierer, S. M., and Bierer, J. A. (**2010**). "Modeling the electrode-neuron interface of cochlear implants: Effects of neural survival, electrode placement, and the partial tripolar configuration," Hear. Res. **268**(1–2), 93–104.

Goupell, M. J. (**2015**). "Interaural envelope correlation change discrimination in bilateral cochlear implantees: Effects of mismatch, centering, and onset of deafness," J. Acoust. Soc. Am. **137**(3), 1282–1297.

Goupell, M. J., Best, V., and Colburn, H. S. (**2021**). "Intracranial lateralization bias observed in the presence of symmetrical hearing thresholds," JASA Express Lett. **1**(10), 104401.

Goupell, M. J., Kan, A., and Litovsky, R. Y. (**2013a**). "Mapping procedures can produce non-centered auditory images in bilateral cochlear implantees," J. Acoust. Soc. Am. **133**(2), EL101–EL107.

Goupell, M. J., Kan, A., and Litovsky, R. Y. (**2016**). "Spatial attention in bilateral cochlear-implant users," J. Acoust. Soc. Am. **140**(3), 1652–1662.

Goupell, M. J., and Litovsky, R. Y. (**2015**). "Sensitivity to interaural envelope correlation changes in bilateral cochlear-implant users," J. Acoust. Soc. Am. **137**(1), 335–349.

Goupell, M. J., Majdak, P., and Laback, B. (**2010**). "Median-plane sound localization as a function of the number of spectral channels using a channel vocoder," J. Acoust. Soc. Am. **127**(2), 990–1001.

Goupell, M. J., Stakhovskaya, O. A., and Bernstein, J. G. W. (**2018**). "Contralateral interference caused by binaurally presented competing speech in adult bilateral cochlear-implant users," Ear Hear. **39**(1), 110–123.

Goupell, M. J., Stoelb, C., Kan, A., and Litovsky, R. Y. (**2013b**). "Effect of mismatched place-of-stimulation on the salience of binaural cues in conditions that simulate bilateral cochlear-implant listening," J. Acoust. Soc. Am. **133**(4), 2272–2287.

Grantham, D. W., Ashmead, D. H., Ricketts, T. A., Haynes, D. S., and Labadie, R. F. (**2008**). "Interaural time and level difference thresholds for acoustically presented signals in post-lingually deafened adults fitted with bilateral cochlear implants using CIS+ processing," Ear Hear. **29**(1), 33–44.

Gray, W. O., Mayo, P. G., Goupell, M. J., and Brown, A. D. (**2021**). "Transmission of binaural cues by bilateral cochlear implants: Examining the impacts of bilaterally independent spectral peak-picking, pulse timing, and compression," Trends Hear. **25**, 1–23.

Greenwood, D. D. (**1990**). "A cochlear frequency-position function for several species—29 years later," J. Acoust. Soc. Am. **87**(6), 2592–2605.

Guinan, J. J., Norris, B. E., and Guinan, S. S. (**1972**). "Single auditory units in the superior olivary complex: II: Locations of unit categories and tonotopic organization," Int. J. Neurol. **4**(4), 147–166.

Hafter, E. R., and Buell, T. N. (**1990**). "Restarting the adapted binaural system," J. Acoust. Soc. Am. **88**(2), 806–812.

Hafter, E. R., and Dye, R. H. (**1983**). "Detection of interaural differences of time in trains of high-frequency clicks as a function of interclick interval and number," J. Acoust. Soc. Am. **73**(2), 644–651.

Henning, G. B. (**1974**). "Detectability of interaural delay in high-frequency complex waveforms," J. Acoust. Soc. Am. **55**(1), 84–90.

Holder, J. T., Reynolds, S. M., Sunderhaus, L. W., and Gifford, R. H. (**2018**). "Current profile of adults presenting for preoperative cochlear implant evaluation," Trends Hear. **22**, 1–16.

Hu, H., Ewert, S. D., McAlpine, D., and Dietz, M. (**2017**). "Differences in the temporal course of interaural time difference sensitivity between acoustic and electric hearing in amplitude modulated stimuli," J. Acoust. Soc. Am. **141**(3), 1862–1873.

Ihlefeld, A., Carlyon, R. P., Kan, A., Churchill, T. H., and Litovsky, R. Y. (**2015**). "Limitations on monaural and binaural temporal processing in bilateral cochlear implant listeners," J. Assoc. Res. Otolarygol. **16**(5), 641–652.

Ihlefeld, A., Kan, A., and Litovsky, R. Y. (**2014**). "Across-frequency combination of interaural time difference in bilateral cochlear implant listeners," Front. Syst. Neurosci. **8**(22), 22.

Ihlefeld, A., and Litovsky, R. Y. (**2012**). "Interaural level differences do not suffice for restoring spatial release from masking in simulated cochlear implant listening," PLoS One **7**(9), e45296.

Javel, E., and Shepherd, R. K. (**2000**). "Electrical stimulation of the auditory nerve in man," Hear. Res. **140**, 45–76.

Jeffress, L. A. (**1948**). "A place theory of sound localization," J. Comp. Physiol. Psychol. **41**(1), 35–39.

Joris, P. X., and van der Heijden, M. (**2019**). "Early binaural hearing: The comparison of temporal differences at the two ears," Annu. Rev. Neurosci. **42**, 433–457.

Joris, P. X., and Yin, T. C. T. (**1992**). "Responses to amplitude-modulated tones in the auditory nerve of the cat," J. Acoust. Soc. Am. **91**(1), 215–232.

Joris, P. X., and Yin, T. C. T. (**1995**). "Envelope coding in the lateral superior olive. I. Sensitivity to interaural time differences," J. Neurophysiol. **73**(3), 1043–1062.

Kan, A., Goupell, M. J., and Litovsky, R. Y. (**2019**). "Effect of channel separation and interaural mismatch on fusion and lateralization in normal-hearing and cochlear-implant listeners," J. Acoust. Soc. Am. **146**(2), 1448–1463.

Kan, A., and Litovsky, R. Y. (**2015**). "Binaural hearing with electrical stimulation," Hear. Res. **322**, 127–137.

Kan, A., Litovsky, R. Y., and Goupell, M. J. (**2015**). "Effects of interaural pitch matching and auditory image centering on binaural sensitivity in cochlear implant users," Ear Hear. **36**(3), e62–e68.

Kan, A., Peng, Z. E., Moua, K., and Litovsky, R. Y. (**2018**). "A systematic assessment of a cochlear implant processor's ability to encode interaural time differences," in *2018 Asia-Pacific Signal and Information Processing Association Annual Summit and Conference (APSIPA ASC)*, Honolulu, HI, pp. 382–387.

Kan, A., Stoelb, C., Litovsky, R. Y., and Goupell, M. J. (**2013**). "Effect of mismatched place-of-stimulation on binaural fusion and lateralization in bilateral cochlear-implant users," J. Acoust. Soc. Am. **134**(4), 2923–2936.

Kenward, M. G., and Roger, J. H. (**1997**). "Small sample inference for fixed effects from restricted maximum likelihood," Biometrics **53**(3), 983–997.

Kirby, B., Brown, C., Abbas, P., Etler, C., and O'Brien, S. (**2012**). "Relationships between electrically evoked potentials and loudness growth in bilateral cochlear implant users," Ear Hear. **33**(3), 389–398.

Klein-Hennig, M., Dietz, M., Hohmann, V., and Ewert, S. D. (**2011**). "The influence of different segments of the ongoing envelope on sensitivity to interaural time delays," J. Acoust. Soc. Am. **129**(6), 3856–3872.

Klug, J., and Dietz, M. (**2022**). "Frequency dependence of sensitivity to interaural phase differences in pure tones," J. Acoust. Soc. Am. **152**(6), 3130–3141.

Klug, J., Schmors, L., Ashida, G., and Dietz, M. (**2020**). "Neural rate difference model can account for lateralization of high-frequency stimuli," J. Acoust. Soc. Am. **148**(2), 678–691.

Laback, B., Egger, K., and Majdak, P. (**2015**). "Perception and coding of interaural time differences with bilateral cochlear implants," Hear. Res. **322**, 138–150.

Laback, B., Zimmermann, I., Majdak, P., Baumgartner, W.-D., and Pok, S.-M. (**2011**). "Effects of envelope shape on interaural envelope delay sensitivity in acoustic and electric hearing," J. Acoust. Soc. Am. **130**(3), 1515–1529.

Landsberger, D. M. (**2008**). "Effects of modulation wave shape on modulation frequency discrimination with electrical hearing," J. Acoust. Soc. Am. **124**(2), EL21–EL27.

Leake, P. A., and Hradek, G. T. (**1988**). "Cochlear pathology of long term neomycin induced deafness in cats," Hear. Res. **33**(1), 11–33.

Lindenbeck, M. J., Majdak, P., and Laback, B. (**2024**). "Effects of monaural temporal electrode asynchrony and channel interactions in bilateral and unilateral cochlear-implant stimulation," Trends Hear. **28**, 1–18.

Litovsky, R. Y., Goupell, M. J., Fay, R. R., and Popper, A. N. (**2021**). *Binaural Hearing* (Springer, Cham, Switzerland).

Litovsky, R. Y., Goupell, M. J., Godar, S., Grieco-Calub, T., Jones, G. L., Garadat, S. N., Agrawal, S., Kan, A., Todd, A., Hess, C., and Misurelli, S. (**2012**). "Studies on bilateral cochlear implants at the University of Wisconsin Binaural Hearing and Speech Lab," J. Am. Acad. Audiol. **23**, 476–494.

Litovsky, R. Y., Jones, G. L., Agrawal, S., and van Hoesel, R. (**2010**). "Effect of age at onset of deafness on binaural sensitivity in electric hearing in humans," J. Acoust. Soc. Am. **127**(1), 400–414.

Loizou, P. C. (**2006**). "Speech processing in vocoder-centric cochlear implants," in *Cochlear and Brainstem Implants*, edited by A. R. Møller (Karger, Basel, Switzerland), Vol. 64, pp. 109–143.

Long, C. J., Holden, T. A., McClelland, G. H., Parkinson, W. S., Shelton, C., Kelsall, D. C., and Smith, Z. M. (**2014**). "Examining the electro-neural interface of cochlear implant users using psychophysics, CT scans, and speech understanding," J. Assoc. Res. Otolarygol. **15**(2), 293–304.

Lord Rayleigh, O. M. P. R. S. (**1907**). "XII. On our perception of sound direction," London, Edinburgh Dublin Philos. Mag. **13**(74), 214–232.

Macpherson, E. A., and Middlebrooks, J. C. (**2002**). "Listener weighting of cues for lateral angle: The duplex theory of sound localization revisited," J. Acoust. Soc. Am. **111**(5), 2219–2236.

Majdak, P., Laback, B., and Baumgartner, W.-D. (**2006**). "Effects of interaural time differences in fine structure and envelope on lateral discrimination in electric hearing," J. Acoust. Soc. Am. **120**(4), 2190–2201.

Mayo, P. G., Saunders, P. C., and Goupell, M. J. (**2021**). "Interaural-time-difference thresholds for broad band-limited pulses are affected by relative bandwidth not temporal envelope sharpness," JASA Express Lett. **1**, 124401.

McAlpine, D., and Grothe, B. (**2003**). "Sound localization and delay lines - Do mammals fit the model?," Trends Neurosci. **26**(7), 347–350.

Monaghan, J. J. M., Bleeck, S., and McAlpine, D. (**2015**). "Sensitivity to envelope interaural time differences at high modulation rates," Trends Hear. **19**, 1–14.

Moore, B. C. J. (**2008**). "The role of temporal fine structure processing in pitch perception, masking, and speech perception for normal-hearing and hearing-impaired people," J. Assoc. Res. Otolarygol. **9**(4), 399–406.

Mosnier, I., Sterkers, O., Bebear, J. P., Godey, B., Robier, A., Deguine, O., Fraysse, B., Bordure, P., Mondain, M., Bouccara, D., Bozorg-Grayeli, A., Borel, S., Ambert-Dahan, E., and Ferrary, E. (**2009**). "Speech performance and sound localization in a complex noisy environment in bilaterally implanted adult patients," Audiol. Neurotol. **14**(2), 106–114.

Nadol, J. J. (**1997**). "Patterns of neural degeneration in the human cochlea and auditory nerve: Implications for cochlear implantation," Otolaryngol. Head. Neck Surg. **117**(3), 220–228.

Noel, V. A., and Eddington, D. K. (**2013**). "Sensitivity of bilateral cochlear implant users to fine-structure and envelope interaural time differences," J. Acoust. Soc. Am. **133**(4), 2314–2328.

Nuetzel, J. M., and Hafter, E. R. (**1981**). "Discrimination of interaural delays in complex waveforms: Spectral effects," J. Acoust. Soc. Am. **69**(4), 1112–1118.

Peters, B. R., Wyss, J., and Manrique, M. (**2010**). "Worldwide trends in bilateral cochlear implantation," Laryngoscope **120**(5), S17–S44.

Poon, B. B., Eddington, D. K., Noel, V., and Colburn, H. S. (**2009**). "Sensitivity to interaural time difference with bilateral cochlear implants: Development over time and effect of interaural electrode spacing," J. Acoust. Soc. Am. **126**(2), 806–815.

Reeder, R. M., Firszt, J. B., Holden, L. K., and Strube, M. J. (**2014**). "A longitudinal study in adults with sequential bilateral cochlear implants: Time course for individual ear and bilateral performance," J. Speech. Lang. Hear. Res. **57**(3), 1108–1126.

Reiss, L. A. J., and Goupell, M. J. (**2024**). "Binaural fusion: Complexities in definition and measurement," J. Acoust. Soc. Am. **156**(4), 2395–2408.

Resnick, J. M., O'Brien, G. E., and Rubinstein, J. T. (**2018**). "Simulated auditory nerve axon demyelination alters sensitivity and response timing to extracellular stimulation," Hear. Res. **361**, 121–137.

Rothman, J. S., Young, E. D., and Manis, P. B. (**1993**). "Convergence of auditory nerve fibers onto bushy cells in the ventral cochlear nucleus: Implications of a computational model," J. Neurophysiol. **70**(6), 2562–2583.

Rule, S. J. (**1994**). "Lateralization of high frequency, amplitude modulated sounds as a function of carrier frequency," Can. J. Exp. Psychol. **48**(3), 435–443.

Saberi, K., Takahashi, Y., Konishi, M., Albeck, Y., Arthur, B. J., and Farahbod, H. (**1998**). "Effects of interaural decorrelation on neural and behavioral detection of spatial cues," Neuron **21**(4), 789–798.

Sammeth, C. A., Brown, A. D., Greene, N. T., and Tollin, D. J. (**2023**). "Interaural frequency mismatch jointly modulates neural brainstem binaural interaction and behavioral interaural time difference sensitivity in humans," Hear. Res. **437**, 108839.

Schvartz-Leyzac, K. C., Holden, T. A., Zwolan, T. A., Arts, H. A., Firszt, J. B., Buswinka, C. J., and Pfingst, B. E. (**2020**). "Effects of electrode location on estimates of neural health in humans with cochlear implants," J. Assoc. Res. Otolarygol. **21**(3), 259–275.

Shannon, R. V., Galvin, J. J., and Baskent, D. (**2002**). "Holes in hearing," J. Assoc. Res. Otolaryngol. **3**(2), 185–199.

Shepherd, R. K., and Hardie, N. A. (**2001**). "Deafness-induced changes in the auditory pathway: Implications for cochlear implants," Audiol. Neurotol. **6**(6), 305–318.

Spoendlin, H., and Schrott, A. (**1989**). "Analysis of the human auditory nerve," Hear. Res. **43**(1), 25–38.

Stecker, G. C. (**2018**). "Temporal weighting functions for interaural time and level differences. V. Modulated noise carriers," J. Acoust. Soc. Am. **143**(2), 686–695.

Stecker, G. C., Bernstein, L. R., and Brown, A. D. (**2021**). "Binaural hearing with temporally complex signals," in *Binaural Hearing*, edited by R. Y. Litovsky, M. J. Goupell, R. R. Fay, and A. N. Popper (Springer International Publishing, Cham, Switzerland), pp. 145–180.

Stellmack, M. A., Viemeister, N. F., and Byrne, A. J. (**2005**). "Discrimination of interaural phase differences in the envelopes of sinusoidally amplitude-modulated 4-kHz tones as a function of modulation depth," J. Acoust. Soc. Am. **118**(1), 346–352.

Stern, R. M., and Shear, G. D. (**1996**). "Lateralization and detection of low-frequency binaural stimuli: Effects of distribution of internal delay," J. Acoust. Soc. Am. **100**(4), 2278–2288.

Stern, R. M., Zeiberg, A. S., and Trahiotis, C. (**1988**). "Lateralization of complex binaural stimuli: A weighted-image model," J. Acoust. Soc. Am. **84**(1), 156–165.

Swaminathan, J., Mason, C. R., Streeter, T. M., Best, V., Roverud, E., and Kidd, G. (**2016**). "Role of binaural temporal fine structure and envelope cues in cocktail-party listening," J. Neurosci. **36**(31), 8250–8257.

Thakkar, T., Anderson, S. R., Kan, A., and Litovsky, R. Y. (**2020**). "Evaluating the impact of age, acoustic exposure, and electrical stimulation on binaural sensitivity in adult bilateral cochlear implant patients," Brain Sci. **10**(406), 406–426.

Todd, A. E., Goupell, M. J., and Litovsky, R. Y. (**2017**). "The relationship between intensity coding and binaural sensitivity in adults with cochlear implants," Ear Hear. **38**(2), e128–e141.

Tollin, D. J., and Yin, T. C. T. (**2002**). "The coding of spatial location by single units in the lateral superior olive of the cat. II. The determinants of spatial receptive fields in azimuth," J. Neurosci. **22**(4), 1468–1479.

van Hoesel, R. J. M. (**2008**). "Observer weighting of level and timing cues in bilateral cochlear implant users," J. Acoust. Soc. Am. **124**(6), 3861–3872.

van Hoesel, R. J. M., Jones, G. L., and Litovsky, R. Y. (**2009**). "Interaural time delay sensitivity in bilateral cochear implant users: Effects of pulse rate, modulation rate, and place of stimulation," J. Assoc. Res. Otolarygol. **10**(4), 557–567.

Whitmer, W. M., Seeber, B. U., and Akeroyd, M. A. (**2014**). "The perception of apparent auditory source width in hearing-impaired adults," J. Acoust. Soc. Am. **135**(6), 3548–3559.

Yin, T. C., and Chan, J. C. (**1990**). "Interaural time sensitivity in medial superior olive of cat," J. Neurophysiol. **64**(2), 465–488.

Yin, T. C. T., Smith, P. H., and Joris, P. X. (**2019**). "Neural mechanisms of binaural processing in the auditory brainstem," Compr. Physiol. **9**(4), 1503–1575.

Zhou, R., Abbas, P. J., and Assouline, J. G. (**1995a**). "Electrically evoked auditory brainstem response in peripherally myelin-deficient mice," Hear. Res. **88**(1–2), 98–106.

Zhou, R., Assouline, J. G., and Abbas, P. J. (**1995b**). "Anatomical and physiological measures of auditory system in mice with peripheral myelin deficiency," Hear. Res. **88**, 87–97.

Zilany, M. S. A., Bruce, I. C., and Carney, L. H. (**2014**). "Updated parameters and expanded simulation options for a model of the auditory periphery," J. Acoust. Soc. Am. **135**(1), 283–286.

Zirn, S., Arndt, S., Aschendorff, A., Laszig, R., and Wesarg, T. (**2016**). "Perception of interaural phase differences with envelope and fine structure coding strategies in bilateral cochlear implant users," Trends Hear. **20**, 1–12.

Zwislocki, J., and Feldman, R. S. (**1956**). "Just noticeable differences in dichotic phase," J. Acoust. Soc. Am. **28**(5), 860–864.